A comprehensive study on the dual species biofilm formation of clinical *Staphylococcus aureus* and *Candida albicans* strains from the same origins

Yaqin Li, Xiang Zhou, Haoyue Xue, Jiaying Hong, Nixuan Gu, Qian Li, Guangchao Yu, Xiaomao Yin, Lei Yuan, Mahesh Premarathna, Xin Lin, Yuzhu Mao, Junyan Liu, Zhenbo Xu

PII: S2590-2075(25)00072-3

DOI: https://doi.org/10.1016/j.bioflm.2025.100324

Reference: BIOFLM 100324

To appear in: *Biofilm*

Received Date: 31 July 2025

Revised Date: 4 October 2025

Accepted Date: 7 October 2025

Please cite this article as: Li Y, Zhou X, Xue H, Hong J, Gu N, Li Q, Yu G, Yin X, Yuan L, Premarathna M, Lin X, Mao Y, Liu J, Xu Z, A comprehensive study on the dual species biofilm formation of clinical *Staphylococcus aureus* and *Candida albicans* strains from the same origins, *Biofilm*, https://doi.org/10.1016/j.bioflm.2025.100324.

A comprehensive study on the dual species biofilm formation of clinical *Staphylococcus aureus* and *Candida albicans* strains from the same origins

Yaqin Li[a, b 1], Xiang Zhou[c1], Haoyue Xue[b], Jiaying Hong[b], Nixuan Gu[b], Qian Li[d], Guangchao Yu[e], Xiaomao Yin[f], Lei Yuan[g], Mahesh Premarathna[h], Xin Lin[b], Yuzhu Mao[i], Junyan Liu [j,k*], Zhenbo Xu [a*]

[a] Department of Laboratory Medicine, the Second Affiliated Hospital of Shantou University Medical College, Shantou 515041, China

[b] School of Food Science and Engineering, Guangdong Province Key Laboratory for Green Processing of Natural Products and Product Safety, Engineering Research Center of Starch and Vegetable Protein Processing Ministry of Education, South China University of Technology, Guangzhou 510640, China

[c] Department of Microsurgery, Trauma and Hand Surgery, The First Affiliated Hospital, Sun Yat-sen University, Guangzhou 510080, China

[d] Center of Clinical Laboratory Medicine, First Affiliated Hospital of Jinan University, Guangzhou 510620, China

[e] Shunde Hospital of Guangzhou University of Chinese Medicine, Foshan, China

[f] Department of Laboratory Medicine, Guangzhou Red Cross Hospital, Jinan University, Guangzhou, China.

[g] School of Food Science and Engineering, Yangzhou University, Yangzhou, Jiangsu, 225127, China

[h] Department of Civil and Environmental Engineering, University of Maryland, College

Park, MD 20742, USA

[i] Microbial Biotechnology Unit, National Institute of Fundamental Studies, Kandy 20000, Sri Lanka

[j] College of Light Industry and Food Science, Guangdong Provincial Key Laboratory of Lingnan Specialty Food Science and Technology, Academy of Contemporary Agricultural Engineering Innovations, Zhongkai University of Agriculture and Engineering, Guangzhou 510225, China

[k] Key Laboratory of Green Processing and Intelligent Manufacturing of Lingnan Specialty Food, Ministry of Agriculture, Guangzhou 510225, China

[1]These authors contribute equally to this study.

*Corresponding author:

Zhenbo Xu, Ph.D., Mailing address: School of Food Science and Engineering, South China University of Technology, Guangzhou 510640, China, Email: zhenbo.xu@hotmail.com

Junyan Liu, Ph.D., Mailing address: College of Light Industry and Food Science, Zhongkai University of Agriculture and Engineering, Guangzhou 510225, China, Email: yaner0722@hotmail.com

Abstract

Biofilms, complex microbial communities that enhance pathogen survival in hostile environments, are integral to chronic infections and often exhibit polymicrobial interactions that influence disease outcomes. Among these, *Staphylococcus aureus* and *Candida albicans* co-infections are of particular clinical significance due to their synergistic mechanisms, resulting in invasive and treatment-resistant infections. This study investigated the interaction dynamics of *S. aureus* and *C. albicans* in both planktonic and biofilm states, focusing on growth dominance, biofilm formation, and structural adaptations under different conditions. Results revealed that *C. albicans* dominated in planktonic co-culture, suppressing *S. aureus* growth, whereas biofilm conditions favored mutual adaptation, with hyphae-competent *C. albicans* forming dual-species biofilms with *S. aureus* that accumulated substantial biomass, thereby enhancing biofilm cohesion and resistance. Compared to yeast cells in YPD, hyphal growth induced by RPMI substrates significantly augmented biofilm formation across the early, proliferating, and mature stages. Colonization order influenced biofilm architecture and interspecies interactions, with highly mature biofilms exhibiting dense network structures and increased *C. albicans* hyphal formation. Mechanical measurements revealed an elastic modulus of up to 10 Pa, indicating enhanced biofilm rigidity and structural integrity. Notably, the hyphal contribution of *C. albicans* was stage-dependent—facilitating *S. aureus* proliferation during proliferating phase. These findings underscore the complexity of *S. aureus*-*C. albicans* interactions and highlight potential targets for disrupting biofilm-associated chronic infections.

Keywords: Polymicrobial infections; biofilm; *S. aureus*; *C. albicans*

1 Introduction

In acute infection, bacteria commonly appear as single cells, whereas in multicellular biofilms they play a crucial role in chronic infections, making infections resistant to adequate antibiotic therapy and host immune defense (M. Burmølle et al., 2010; Costerton, Stewart, & Greenberg, 1999; Høiby et al., 2015; Hoiby et al., 1977). Additionally, most biofilms in the environment grow as polymicrobial biofilms which encase diverse microorganisms to protect against the hostile conditions (Mette Burmølle et al., 2010; Stoodley, Sauer, Davies, & Costerton, 2002; Willems, Xu, & Peters, 2016). Compared to single-microbe, interactions such as antagonism or synergy between polymicrobial infections may be linked to more severe outcomes and alter the course of the illness (Brogden, Guthmiller, & Taylor, 2005; Gabrilska & Rumbaugh, 2015; Wolcott, Costerton, Raoult, & Cutler, 2013). Therefore, it is crucial to study how the presence of pathogens in polymicrobial infections influences microbial interactions. From symbiotic microbial communities, bacteria and fungi are frequently co-isolated, where they directly or indirectly influence each other in various ways (Carlson, 1982; Paul et al., 2024; Peleg, Hogan, & Mylonakis, 2010). *Candida albicans*, an opportunistic fungus widely distributed on human mucosal surfaces, and *Staphylococcus aureus*, a common bacterial pathogen, can cause nosocomial infections with high mortality rates, and their interactions often result in invasive diseases that are difficult to treat. A unique intra-abdominal interaction between the host and *S. aureus* - *C. albicans* infection leads to intense inflammatory responses, pathogen dissemination, and fatal sepsis, regardless of *C. albicans* morphogenesis (Nash, Peters, Palmer, Fidel,

& Noverr, 2014). In mixed infections, *S. aureus* adheres to and encapsulates *C. albicans*, and in the presence of neutrophils, the outer layer of *S. aureus* is preferentially killed, while *S. aureus* simultaneously promotes the proliferation and hyphal growth of *C. albicans* (Jing et al., 2024). The cooperative evasion strategy between *S. aureus* and *C. albicans* enhances their co-infection invasiveness, allowing both pathogens to more effectively resist the host's immune defense(Allison et al., 2019; T. Y. Shao et al., 2019; Van Dyck et al., 2021). Recent proteomic and transcriptomic studies further demonstrated that *C. albicans* and *S. aureus* reciprocally promoted the secretion of extracellular virulence factors and enhanced pro-inflammatory responses in macrophages, providing mechanistic insights into the elevated morbidity and mortality associated with their co-infections (Pasman et al., 2025).

Despite these advances, the precise mechanisms by which *S. aureus* and *C. albicans* coordinate during polymicrobial infections remain incompletely understood, particularly regarding shifts in dominance, biofilm architecture, and structural resilience. Therefore, the objective of this study was to further clarify the mechanisms driving microbial interactions during *S. aureus* - *C. albicans* polymicrobial infections, with a particular focus on the shifts in dominance, biofilm formation, and structural adaptations in both planktonic and biofilm states. Our findings demonstrated that *S. aureus* could combine with *C. albicans* hyphae in mature biofilms, which contributed to enhanced network cohesion and shear resistance. These results highlight the complex and synergistic relationship between *S. aureus* and *C. albicans*, emphasizing the importance of structural and mechanical adaptations in polymicrobial biofilm

persistence, which may offer potential targets for disrupting chronic infections in clinical settings.

2 Materials and methods

2.1 Strains and growth conditions

In this study, the strains included 24 pairs of *C. albicans* and *S. aureus* co-isolated from clinical specimens collected from the same site of the same patient at the First Affiliated Hospital of Jinan University between April 2019 and January 2020, along with 3 *S. aureus* strains isolated from clinical sources (Table 1). The standard strains used were *C. albicans* SC5314 and *S. aureus* ATCC25923. All strains were stored in 20% glycerine at -80°C refrigerator. A small volume of glycerol stock was plated onto 1.5% agar and incubated under optimal conditions (30°C for 24 hours for *C. albicans* and 37°C for 24 hours for *S. aureus*) to isolate single colonies. A single colony was transferred into 2 mL of the suitable broth and incubated overnight at the optimal temperature with shaking at 200 rpm prior. The overnight culture was transferred to a centrifuge tube and centrifuged at 5,000 rpm for 1 minute. The supernatant was discarded, and the cells were washed twice with PBS. The cells were resuspended in 2 mL of RPMI (Sigma-Aldrich, USA) or YPD medium (Huankai, China). Subsequently, *S. aureus* and *C. albicans* were diluted in YPD or RPMI medium at a specific ratio to obtain a final concentration of 10^6 CFU/mL for subsequent experiments.

2.2 Preparation of microbial Co-culture

2.2.1 Polymicrobial interaction of *S. aureus*-*C. albicans* in planktonic

Three groups were established: *C. albicans* monoculture, *S. aureus* monoculture, and *S.*

aureus–C. albicans co-culture. Cultures were incubated in RPMI medium at 37 °C with agitation at 200 rpm to maintain planktonic growth conditions. Culturable cells were subsequently monitored at 8, 16, 24, 48, 72, and 120 h.

2.2.2 Dual species biofilm of *S. aureus* and *C. albicans* in hyphal or yeast forms

To investigate how hyphal morphologies of *C. albicans* under different nutrient conditions influence its interaction with *S. aureus*, biofilm models were established in both YPD and RPMI media. Separate 96-well plates were prepared for each group, time point, and method, with 100 μL of culture in each well. Corresponding *S. aureus* and *C. albicans* strains (e.g., Sa-1 and Ca-1) were co-inoculated into the wells at a 1:1 volumetric ratio, representing paired co-isolated strains. Plates were incubated at 37 °C for 24, 72, and 168 h. The medium was replaced with fresh media every 48 h. At each time point, planktonic cells were removed, and the wells were washed three times with 200 μL PBS to eliminate non-adherent cells. Biofilm cells were then recovered by adding 100 μL saline and scraping the well bottoms and walls with pipette tips, repeated three times to yield 300 μL of biofilm suspension. The suspension was vortexed for 2 min and subsequently subjected to colony counting.

2.2.3 Dual-species biofilm model with varying initial *S. aureus–C. albicans* ratios

The initial ratios of *C. albicans* and *S. aureus* were adjusted to the following combinations: 1:1000 and 1:10 (final concentrations of 10^3 CFU/mL and 10^6 CFU/mL, respectively), 1:1000 and 1:100 (10^3 CFU/mL and 10^5 CFU/mL, respectively), 1:100 and 1:100 (10^4 CFU/mL and 10^5 CFU/mL, respectively), 1:10 and 1:100 (10^5 CFU/mL and 10^5 CFU/mL, respectively), 1:10 and 1:1000 (10^5 CFU/mL and 10^4 CFU/mL,

respectively). 50 μL of each prepared suspension were added into a 96-well plate (final volume: 100 μL) and incubated under the specified conditions for 24 h (early biofilm phase), 72 h (proliferating biofilm phase), and 168 h (mature biofilm phase). The medium was refreshed every 48 h. Three independent replicates were performed for each experiment to ensure reproducibility.

2.2.4 Dual-species biofilm model with varying matrix

The establishment of a polymicrobial biofilm culture model under different biofilm matrix conditions was conducted as follows: *S. aureus* was diluted at a ratio of 1:1000, and *C. albicans* at a ratio of 1:100. Two 96-well culture plates were prepared, with the appropriately diluted *S. aureus* and *C. albicans* inoculated into separate wells. Initial incubation times were set at 4 h, 8 h, 24 h, and 48 h. At the corresponding time points, the plates were removed, and *C. albicans* was introduced into the wells containing *S. aureus*, while *S. aureus* was introduced into the wells containing *C. albicans*, to establish polymicrobial biofilm models under varying matrix conditions. Plates were incubated at 37 °C for 24, 72, and 168 h. The medium was replaced with fresh media every 48 h. The experiments were performed in triplicate for reproducibility.

2.2.5 Polymicrobial biofilm model with *C. albicans* of varying hyphal ability

The standard *C. albicans* strain SC5314, together with nine clinical isolates representing three isolates each of strong, medium, and weak hyphal-forming ability, were co-cultured with *S. aureus*. Monoculture of *S. aureus* were included as control. Corresponding *S. aureus* and *C. albicans* strains were co-inoculated into 96-well plates at a 1:1 volumetric ratio, with 200 μL of culture per well. Separate plates were prepared

for each group and time point. Plates were incubated at 37 °C for 24, 72, and 168 h. Fresh medium was added to the wells every 48 h.

2.2.6 Mature Dual-species biofilm model for amplitude sweep

Three clinical *C. albicans* isolates, representing one isolate each with strong, medium, or weak hyphal-forming ability, were co-cultured with *S. aureus* strains exhibiting strong, medium, or weak biofilm-forming capacity, generating a total of nine experimental groups. Corresponding *S. aureus* and *C. albicans* strains were co-inoculated into 24-well plates at a 1:1 volumetric ratio, with 1 mL of culture per well. Plates were incubated in 5% TSB at 35°C for 48 h, followed by dehydration at room temperature (22–25°C) for an additional 48 h. Subsequently, three cycles of growth in 5% TSB for 6 h were conducted, each followed by extended dehydration periods of 66, 42, and 66 h at room temperature. Controls, representing non-mature biofilms, were maintained in parallel, with the medium replaced every 48 h.

2.3 Colony Forming Units determination

At specific time points (0 h, 8 h, 16 h, 24 h, 48 h, 72 h, and 5 days), 100 μL of culture was sampled from each group (*C. albicans* monoculture, *S. aureus* monoculture, and *S. aureus* + *C. albicans* coculture). The samples were serially diluted, and 10 μL of the appropriate dilution was plated onto selective agar for colony enumeration. For the *C. albicans* monoculture, selective YPD agar containing 200 μg/mL chloramphenicol was used. For the *S. aureus* monoculture, selective TSA agar containing 10 μg/mL amphotericin B was utilized. For the coculture, samples were plated on both selective YPD agar and selective TSA agar to distinguish fungal and bacterial populations. YPD

agar plates were incubated at 30°C for 2 days, while TSA agar plates were incubated at 37°C for 1 day until colonies were countable.

2.4 Crystal Violet test

The crystal violet staining method, a standard technique for quantifying biofilm biomass, relies on crystal violet's ability to stain intracellular nucleic acids deep purple, differentiating microbial cells from the background (Xu et al., 2016). In this study, biofilms were grown in 96-well plates, washed with PBS to remove planktonic cells, and stained with 125 μL of crystal violet solution for 10 minutes. After washing the wells with water and air-drying, 200 μL of 95% ethanol was added to dissolve the stain, and 125 μL of the eluate was transferred to a new plate for absorbance measurement at 570 nm. The biofilm biomass was calculated by subtracting the negative control OD. Based on Stepanovic's criteria (Stepanović et al., 2007), biofilm formation was classified as weak ($0 < SI \leq 2$), moderate ($2 < SI \leq 4$), or strong ($SI > 4$), with SI derived as the ratio of sample OD to the critical OD (ODc = mean control OD + 3×SD).

2.5 Rheometry

The rheological properties of the biofilm were measured using an MCR Evolution rheometer in strain-controlled mode. Mature biofilms were gently scraped from plates using a glass slide, and the aggregates were placed on the sample stage of the rheometer for amplitude sweep testing. Under constant gap height and steady conditions, amplitude sweeps were conducted over a strain range of 0.001% to 1000% at a fixed angular frequency (ω).

2.6 Statistical analysis

Data analysis was performed using GraphPad Prism 9.5.0, with results expressed as mean ± standard deviation. Tukey's multiple comparison test was used to compare the mean values of each column with those of other columns. A p-value of <0.05 was considered statistically significant. The p-value notations were as follows: GP: 0.1234 (ns), 0.0332 (*), 0.0021 (**), 0.0002 (***), and <0.0001 (****).

3 Results

3.1 Polymicrobial interaction of *S. aureus*-*C. albicans* in planktonic (acute infection) -- *C. albicans* dominance in co-culture

Acute infections are mostly associated with planktonic cells. To investigate the interactions between *S. aureus* and *C. albicans* under these conditions, we monitored the CFU-based growth curves of 24 isolate pairs over a 0–120 h period (Figure S1). In monocultures, most *S. aureus* isolates (e.g., Sa1, Sa2, Sa21) proliferated rapidly, exceeding 10^8 CFU/mL within the first 24 h. By contrast, *C. albicans* monocultures generally remained below 10^8 CFU/mL. In co-cultures, *S. aureus* growth was consistently suppressed compared with the corresponding monocultures. For example, Sa1+Ca1, Sa2+Ca2, and Sa21+Ca21 showed significantly lower *S. aureus* CFU counts at nearly all time points up to 120 h. Some pairs displayed delayed effects. Sa19+Ca19, for instance, showed no early differences but exhibited clear suppression at 120 h. The growth of *C. albicans* was largely unaffected by co-culture. Its CFU counts remained similar to monocultures throughout the experiment. A few minor exceptions were observed. In Sa3+Ca3, monocultured *C. albicans* had slightly higher counts at 16 h, and in Sa22+Ca22, this difference appeared at 72 h. Taken together, these results

demonstrated that in the planktonic model, *C. albicans* exerted a dominant inhibitory effect on *S. aureus* proliferation, while the growth of *C. albicans* itself remained largely stable and unaffected by *S. aureus*.

3.2 Dual species biofilm of *S. aureus* and *C. albicans*

While the planktonic co-culture analysis demonstrated that *C. albicans* suppressed *S. aureus* proliferation, the interaction dynamics shifted considerably under biofilm conditions, which are more representative of chronic infections. Biofilms provide a protective environment that could alter microbial interactions, and factors such as the sequence of colonization and the nutrient availability in different biofilm locations may further influence the growth and dominance of *S. aureus* and *C. albicans*.

To better understand how these factors affected dual-species biofilm development, we selected two nutrient substrates, YPD, which promotes yeast growth, and RPMI, which indicates hyphal growth, to construct a coexisting biofilm model of *S. aureus* and *C. albicans*, focusing on the dynamic diversity during the biofilm formation process (Ma et al., 2022). This model allowed us to examine the impact of *C. albicans* morphotypes on interspecies interactions, as well as the roles of colonization order (reflected by initial inoculation concentration) and growth order (which shapes the biofilm matrix) in determining biofilm structure and composition. The following sections present a detailed analysis of dual-species biofilms formed under yeast and hyphal conditions, a comparison of these two morphotypes, and an exploration of how initial inoculation and colonization sequence affect the dynamics of dual-species biofilm formation.

3.2.1 Dual species biofilm of *S. aureus* and *C. albicans* (in yeast cells)

To monitor the dynamics of biofilm development, we measured the biomass of mono- and dual-species biofilms of *C. albicans* (yeast form) and *S. aureus* at 24, 72, and 168 h using the crystal violet assay. At the early biofilm stage, all 24 coexisting isolates and standard strains formed weak biofilms in dual culture when *C. albicans* was in the yeast state (Table S1), as classified by biofilm-forming capacity criteria (Stepanović et al., 2007). In mono-cultures, *C. albicans* biofilms also showed uniformly weak biomass, whereas *S. aureus* biofilms displayed heterogeneous capacities, with most isolates remaining weak but a subset (e.g., Sa4, Sa8, Sa9) exhibiting medium-level biomass. Proliferating biofilm was accompanied by the formation of microcolony structures, which provide increased surface area for nutrient exchange and waste removal, while also facilitating the dissemination of biofilm-associated cells to distal sites (Moormeier & Bayles, 2017). At the proliferating stage, dual-species biofilms still largely exhibited weak biomass accumulation under yeast cell conditions. In contrast, mono-*S. aureus* biofilms displayed more dynamic changes: several isolates (e.g., Sa1, Sa2, Sa3, Sa6, Sa7) increased biomass, while others, such as Sa9, displayed the opposite trend. In the mature biofilm, activated Agr-mediated quorum sensing initiates biofilm matrix regulation and cell detachment through protease activation and/or PSM production (Moormeier & Bayles, 2017). At the mature stage, dual-species biofilms revealed greater heterogeneity. One isolate (Sa6) developed strong biomass when cocultured with yeast-form *C. albicans*, whereas the majority (79%, 19/24) remained weak, and only 17% (4/24) and 4% (1/24) reached moderate and strong levels, respectively (Table S1). For mono-cultures, *C. albicans* biofilms remained weak, with only a single isolate

(Ca18) reaching moderate biomass, while *S. aureus* biofilms continued to show isolate-dependent variation. Overall, these findings indicated that when *C. albicans* remained in the yeast state, dual-species biofilms generally failed to accumulate substantial biomass throughout development.

3.2.2 Dual species biofilm of *S. aureus* and *C. albicans* (in hyphae)

Biofilm biomass and culturable cells were quantified for hyphal *C. albicans*, *S. aureus*, and their co-cultures at 24, 72, and 168 h (Figure 1, Table S2). In the early biofilm stage, only one *C. albicans* isolate displayed very strong biomass accumulation in mono-culture across all stages, while the majority showed moderate ability. In contrast, dual-species biofilms did not typically develop strong accumulation (Table S2). Compared with mono-culture, several *C. albicans* isolates (Ca1, Ca2, Ca3, Ca5, Ca6, Ca11) showed higher biomass in co-culture with *S. aureus*, and this trend persisted at 72 h and 168 h (Figure 1). However, exceptions were also evident: at 168 h, isolates such as Ca20 and SC5314 accumulated less biomass in co-culture than in mono-culture (Figure 1). For *S. aureus*, at 24 h, co-culture with hyphal *C. albicans* supported higher biomass than mono-culture in many strains (e.g., Sa1, Sa3, Sa5, Sa6, Sa7, Sa8, Sa10, Sa11, Sa12, Sa14, Sa15, Sa18, Sa19, Sa20, Sa21, Sa23, Sa24). Culturable cell counts at 24 h revealed that co-culture increased recoverable *S. aureus* in several strains (Sa7, Sa11, Sa15, Sa17, Sa18, Sa19, Sa22), whereas *C. albicans* showed a less consistent pattern, with only Ca12 yielding higher counts in co-culture, while Ca4 and Ca11 yielded fewer. During the proliferating biofilm phase, biomass accumulation of *S. aureus* in co-culture remained higher than in mono-culture for multiple isolates (Sa1, Sa2, Sa3, Sa5, Sa6,

Sa9, Sa10, Sa11, Sa17), although culturable cell numbers did not show notable differences. For *C. albicans* at 72 h, only a subset of isolates (Ca1, Ca2, Ca3, Ca5, Ca6, Ca11) displayed increased biomass in co-culture, whereas most isolates showed comparable levels to mono-culture. In mature biofilms, the co-culture condition continued to support greater biomass for many combinations, such as Sa1, Sa2, Sa3, Sa5, Sa6, Sa7, and Sa8 with *C. albicans* in hyphae. Nevertheless, at 168 h, isolates such as Ca20 and SC5314 accumulated more biomass in mono-culture than in co-culture (Figure 1). Culturable cell counts at 168 h generally showed no major differences between conditions, except for Ca7, Ca15, Ca16, and Ca19, where *C. albicans* recovery was higher in mono-culture, and Sa7, where *S. aureus* recovery was higher in co-culture. Across all stages, hyphal *C. albicans* generally was observed to promote *S. aureus* biofilm biomass, particularly in the early adhesion phase, although strain-dependent variability and stage-specific exceptions were consistently observed.

3.2.3 Comparison of dual species biofilm of *S. aureus-C. albicans* in yeast and hyphae

Based on these observations, we compared dual-species biofilms formed with yeast- versus hyphae-state *C. albicans*. Biofilm biomass and culturable cells were measured at 24, 72 and 168 h (Figure 2). The morphological transition of *C. albicans* strongly influenced dual-species architecture. During early biofilm phase, most isolate pairs (71%) produced significantly greater total biomass when *C. albicans* was in the hyphal state than when in the yeast form (e.g., Sa1, Sa2, Sa3, Sa6, Sa7, Sa8, Sa9, Sa13, Sa15, Sa16, Sa17, Sa18, Sa19, Sa20, Sa21, Sa23, Sa24) (Figure 2). Consistently, 24 h CFU

counts showed higher recoverable *S. aureus* in several hyphal co-cultures (Sa1, Sa5, Sa7, Sa10, Sa15, Sa17, Sa18, Sa23). By contrast, *C. albicans* culturable counts at 24 h were generally unchanged by morphology, with only a few isolates (Ca2, Ca4, Ca11, Ca23) showing greater recovery in the yeast form. In the proliferation phase, biomass advantages of hyphal co-culture persisted for multiple *S. aureus* isolates (Sa2, Sa3, Sa6, Sa13, Sa20, Sa23), and no strain pair showed larger biomass with yeast-form *C. albicans*. At 72 h in dual-species biofilms, approximately one-third of *S. aureus* strains (~33%, 8/24) exhibited significantly higher CFU when co-cultured with hyphal *C. albicans*, whereas for *C. albicans*, no significant differences in CFU were observed between the hyphal and yeast states. During the mature biofilm phase, 21 of the 24 co-isolated *S. aureus* strains formed greater total biomass when co-cultured with hyphal *C. albicans*, with 7 strains (33%; e.g., Sa1, Sa8, Sa9, Sa11, Sa12, Sa17, Sa21) exhibiting statistically significant differences. In contrast, culturable cell counts of *S. aureus* showed little variation between the two *C. albicans* morphotypes, with only Sa3 yielding higher recovery in co-culture with hyphal *C. albicans*. Interestingly, for *C. albicans*, the opposite trend was observed: in 168 h dual-species biofilms, more isolates yielded higher CFU in the yeast form than in the hyphal form (e.g., Ca7, Ca10, Ca11, Ca12, Ca13, Ca16, Ca17, Ca19, Ca20, Ca24, and SC5314). In summary, the morphological state of *C. albicans* affected *S. aureus* biofilm formation, with hyphal cells generally promoting dual-species biofilm biomass. This effect was most evident during the early biofilm stage, whereas its influence on *S. aureus* culturable cells was variable, indicating that higher biomass can be achieved without necessarily increasing

bacterial proliferation.

3.3 Influence of initial inoculation concentration on dual species biofilm of *S. aureus* and *C. albicans*

Based on the observed strain- and morphology-dependent effects, a population biofilm model was employed to assess how varying the initial ratios of *S. aureus* and *C. albicans* influenced biofilm. During the early biofilm phase, under the dominance of *S. aureus*, 84% (21/25) of the coexisting *S. aureus* and *C. albicans* combinations formed weak biofilms, while only 16% (4/25) formed moderate biofilms (Table S3). As the inoculum of *C. albicans* increased, the proportion of moderate and strong biofilm producers also rose (Figure S2). Notably, when the difference in inoculum was only one order of magnitude (10^4Ca-1 + 10^5Sa-1), strong biofilms began to appear (4%, 1/25), and under maximum *C. albicans* advantage (10^5Ca-1 + 10^4Sa-1), 28% (7/25) of the coexisting *S. aureus* and *C. albicans* combinations exhibited strong biofilm formation capacity. During the proliferating biofilm phase, most (24/25) co-cultures exhibited an increase in total biofilm biomass as the growth advantage of *C. albicans* progressively strengthened (Figure 3). Unlike the early biofilm, co-cultures formed only weak biofilms under conditions of maximum *S. aureus* growth advantage. As the growth advantage of *S. aureus* diminished, the proportion of coexisting strains capable of forming moderate biofilms gradually increased (Table S3, Figure S2). In the mature biofilm phase, a similar pattern was observed, with total biomass increasing alongside *C. albicans* advantage. Significant differences were found in isolates such as Ca-3+Sa-3, Ca-6+Sa-6, Ca-15+Sa-15, and Ca-17+Sa-17 (Figure 3, Figure S2). Consistent with

the previous observations, *S. aureus* exhibited a stronger proliferative capacity than *C. albicans* under the various growth advantage combinations. In summary, these findings suggested that *C. albicans* promoted *S. aureus* biofilm formation, particularly when bacterial growth advantage is limited, highlighting a cooperative interaction in dual-species biofilms.

3.4 Influence of growth order on dual species biofilm of *S. aureus* and *C. albicans*

To examine the influence of biofilm matrix composition on polymicrobial biofilm formation, *S. aureus* or *C. albicans* was pre-cultured for different durations (4, 8, 24, or 48 h) before introducing the second species, creating distinct matrix conditions for subsequent biofilm development (Figure 4). During the early biofilm phase, as either *S. aureus* or *C. albicans* matrix matured, a larger proportion of dual-species biofilms showed weak biomass accumulation (Figure S3A, Table S4). Strain-dependent effects were evident: for example, Ca-2+Sa-2 exhibited significantly higher biomass on the 8 h *S. aureus* matrix, Ca-4+Sa-4 on the 24 h *C. albicans* matrix, and Ca-12+Sa-12, Ca-23+Sa-23, and Ca-24+Sa-24 on the 4 h *C. albicans* matrix. In contrast, some combinations were largely unaffected by matrix variation, producing consistently low (e.g., Ca-1+Sa-1, Ca-13+Sa-13, Ca-14+Sa-14) or high (e.g., Ca-7+Sa-7, Ca-19+Sa-19, Ca-20+Sa-20) biomass (Figure 4). Culturable cell counts revealed that *C. albicans* was influenced by matrix conditions in 15 strain pairs, while *S. aureus* showed significant differences only in Ca-2+Sa-2 across the 4 h and 8 h *S. aureus* matrix. During the proliferating biofilm phase, a similar trend was observed, with an increasing proportion of weak dual-species biofilm formation as either *S. aureus* or *C. albicans* matrix

matured (Figure S3B, Table S4). The presence of a *C. albicans* matrix promoted biomass accumulation (Ca-8+Sa-8, Ca-18+Sa-18, Ca-20+Sa-20, and Ca-22+Sa-22) showed significantly enhanced biomass on the 8 h *C. albicans* matrix, while Ca-4+Sa-4 also displayed higher biomass on the 24 h matrix. In contrast, some strain pairs (e.g., Ca-13+Sa-13, Ca-14+Sa-14) consistently exhibited weak biofilm, and others (e.g., Ca-7+Sa-7, Ca-23+Sa-23) accumulated a lot of biomass without significant differences, unaffected by the matrix. Culturable cell analysis revealed that *C. albicans* populations were matrix-sensitive in 15 strain pairs, whereas in the remaining cases (e.g., Ca-1+Sa-1, Ca-2+Sa-2, Ca-3+Sa-3), no significant variation was detected. By contrast, *S. aureus* populations were largely unaffected, with only Ca-2+Sa-2 showing significant differences between the 4 h and 8 h *S. aureus* matrix. In the mature biofilm phase, strain-dependent differences were evident. For example, Ca-4+Sa-4 and Ca-5+Sa-5 showed consistently low biomass across different matrix conditions, whereas Ca-7+Sa-7 and Ca-10+Sa-10 exhibited higher levels. Significant increases in total biomass were observed for Ca-3+Sa-3, Ca-7+Sa-7, and Ca-8+Sa-8 on the 8 h *C. albicans* matrix, while Ca-10+Sa-10 and Ca-17+Sa-17 peaked on the 4 h matrix. As the pre-formation time of *C. albicans* matrix increased, the proportion of dual-species biofilms with weak ability gradually increased, although one strain pair still maintained strong biomass under the 8 h condition. Whereas 24 h pre-formation of *S. aureus* matrix was associated with the greatest proportion of weak dual-species biofilms, 4 h pre-formation favored strong biofilm development. (Figure S3C). Regarding culturable cells, *C. albicans* populations were significantly affected by matrix conditions in 17 strain pairs (e.g., Ca-

1+Sa-1, Ca-3+Sa-3, Ca-4+Sa-4), while *S. aureus* was influenced in only six (e.g., Ca-2+Sa-2, Ca-7+Sa-7). In summary, early-stage *C. albicans* matrix was observed to be more favorable for dual-species biomass accumulation, and within these biofilms, *C. albicans* populations were more sensitive to matrix conditions than *S. aureus*.

3.5 Influence of *C. albicans* hyphal on polymicrobial biofilm composition

Throughout the early, proliferating, and mature biofilm phases, polymicrobial biofilms formed by *C. albicans* and *S. aureus* consistently exhibited greater biofilm-forming capacity than those formed by either species alone (Table S1, S2). Moreover, previous observations indicated that differences in *C. albicans* strains—potentially leading to variations in hyphal formation—could differentially affect the growth of *S. aureus* within polymicrobial biofilms. To explore this further, we selected *C. albicans* strains exhibiting distinct hyphal morphologies to co-culture with *S. aureus* and examined the resulting polymicrobial biofilms to assess the proliferation status of *S. aureus*. During the early biofilm formation, *S. aureus* culturable cell counts showed no significant differences between mono-cultures and co-cultures with strongly hyphae-forming *C. albicans*, both reaching 7 log CFU/mL (Figure 5A). In contrast, six weak- or medium-hyphae *C. albicans* strains significantly suppressed *S. aureus* growth, with one exception. The reference strain *C. albicans* SC5314 also inhibited *S. aureus*. During the proliferating biofilm phase, three strong-hyphae *C. albicans* strains significantly enhanced *S. aureus* proliferation, increasing counts by nearly 1 log CFU/mL, while two medium-hyphae strains also promoted bacterial growth (Figure 5B). Among the three weak-hyphae strains, two had no evident effect, whereas one exerted a strong inhibitory

effect. In the mature biofilm phase, only one strong-hyphae strain and the standard strain SC5314 promoted *S. aureus* growth, while the remaining two strong-hyphae strains had no clear effect (Figure 5C). Conversely, two of the three weak-hyphae strains displayed significant inhibitory activity against *S. aureus*. In summary, strong-hyphae strains generally promoted *S. aureus* proliferation, though this effect was not consistently maintained across all biofilm phases, whereas weak-hyphae strains more often exerted inhibitory effects. These findings suggested that the hyphal formation capacity of *C. albicans* differentially influenced its scaffold role in polymicrobial biofilms, thereby affecting the proliferation dynamics of *S. aureus*.

3.6 Shear resistance of mature biofilms

To evaluate how the interplay between *C. albicans* hyphal-forming capacity and *S. aureus* biofilm-forming ability influences the structural properties of mature dual-species biofilms, we performed amplitude sweep analysis. This approach assessed their resistance to shear forces, providing insights into the density, cohesion, and mechanical robustness of the biofilm networks under external stress. Specifically, dual-species biofilms formed by strong-hyphae *C. albicans* with *S. aureus* strains of strong or moderate biofilm-forming ability reached G′ values approaching 10 Pa (Figure 6A–B), with Linear Viscoelastic Region (LVR), indicating high stability. In contrast, when strong-hyphae *C. albicans* was paired with weak biofilm-forming *S. aureus*, shear resistance performed low (G′ < 1 Pa, Figure 6C). Biofilms involving moderate-hyphae *C. albicans* with moderate *S. aureus* displayed lower G′ compared to strong-hyphae combinations, whereas interestingly, weak-hyphae *C. albicans* paired with strong *S.*

aureus achieved G′ values exceeding 10 Pa (Figure 6G). These findings demonstrated that the structural robustness of mature dual-species biofilms arose from the combined contributions of *C. albicans* hyphal ability and *S. aureus* biofilm-forming capacity, both of which shape their resistance to shear stress and overall stability. Nevertheless, overall, mature dual-species biofilms exhibited dense network structures with extended LVR regions, reflecting strong resilience against shear stress.

Discussion

C. albicans can infect various environments within the human body, and its virulence state varies depending on the environmental conditions (Heitman, 2006; Odds, 1988). Factors including pH, CO_2, and N-acetylglucosamine (GlcNAc) can induce the transition of *C. albicans* from yeast to hyphal form, thereby influencing its virulence expression and leading to different infection outcomes(Lu, Su, Solis, Filler, & Liu, 2013; Vylkova et al., 2011; Yang, Zhang, Su, Dong, & Lu, 2023). Polymicrobial biofilm formation was generally enhanced under nutrient-rich conditions that promoted *C. albicans* hyphal growth. This is consistent with reports that hyphal morphogenesis depends on iron availability and provides a structural scaffold for bacterial attachment (Luo et al., 2021; Harriott & Noverr, 2009). Hyphae-associated biofilms are also known to increase *S. aureus* antibiotic tolerance and virulence (Kean et al., 2017; Kong Eric et al., 2016; Schlecht et al., 2015; Todd Olivia et al., 2019). However, not all strain combinations conformed to this trend. For instance, in the Ca-14 + Sa-14 pair, *S. aureus* proliferation was more efficient with yeast-form *C. albicans* (Figure 2). These findings indicated that hyphal presence is not universally advantageous. In addition to nutrient

competition or inhibitory metabolite production, another possibility is that certain *C. albicans* strains have intrinsically weak hyphal-forming ability, resulting in almost no difference in total biofilm biomass between yeast- and hyphae-inducing conditions.

Colonization order further shaped interspecies dynamics. When *C. albicans* was established first, polymicrobial biofilms generally accumulated more efficiently, though the magnitude of this effect varied among strain combinations. Interestingly, *in vivo* studies have shown opposite outcomes, with prior *C. albicans* colonization enhancing host resistance to *S. aureus* (Shao et al., 2019). This discrepancy highlights that microbial interactions observed *in vitro* may not fully capture immune-mediated effects *in vivo*. Colonization sequence thus needed to be interpreted within ecological context, where both microbial competition and host responses jointly determine infection outcomes.

Hyphal capacity played a dual role in biofilm development. Robust hyphae consistently facilitated *S. aureus* colonization by providing physical scaffolds, particularly during the accumulation phase. By contrast, weak-hyphae strains often failed to support—or even inhibited—*S. aureus* proliferation, suggesting antagonistic effects possibly mediated by nutrient competition or secretion of inhibitory metabolites. These findings indicated that *C. albicans* was not merely a passive scaffold but could function either as a facilitator or competitor, depending on strain background and biofilm stage. This further highlights the dual role of *C. albicans* as both a structural and competitive agent in polymicrobial settings. Mature polymicrobial biofilms exhibited high mechanical strength and shear resistance. Such cohesion likely arose from hyphal networks that

464 stabilize the matrix and facilitate *S. aureus* integration (Chow et al, 2021; Lu, Su, Wang,
465 & Liu, 2011). Consistent with this, Vila et al demonstrated that *C. albicans* enhanced *S.*
466 *aureus* tolerance to vancomycin *in vivo* by promoting extracellular matrix production,
467 underscoring the clinical relevance of dense fungal–bacterial biofilm structures (Vila et
468 al., 2021).
469 The findings from this study highlighted the dynamic interactions between *S. aureus*
470 and *C. albicans* in both planktonic and biofilm states, revealing significant shifts in
471 dominance and structural adaptation depending on the growth environment. In
472 planktonic co-culture, *C. albicans* exhibited a dominant inhibitory effect on *S. aureus*
473 proliferation, likely due to the absence of hyphal structures, which limited adhesion and
474 further growth of *S. aureus*. However, in biofilms, this dynamic shifted, as the
475 protective environment and structural network of the biofilm facilitated more complex
476 interactions. Nutrient availability and colonization order were found to significantly
477 influence the biofilm composition and microbial dominance, with nutrient-limited
478 conditions promoting tighter interactions. In matured biofilms, *S. aureus* demonstrated
479 enhanced resistance to mechanical disruption, as shown by amplitude sweep tests,
480 suggesting a denser and more cohesive biofilm structure. Nevertheless, it should be
481 acknowledged that the rheological measurements were performed on biofilms scraped
482 from glass slides, a procedure that may partially alter the hydration state and disrupt the
483 extracellular matrix. While this limitation may affect the absolute values of G′, the
484 relative comparisons between groups remain valid and informative. These findings
485 emphasized the synergistic relationship between *S. aureus* and *C. albicans* in chronic

infection models, where structural and mechanical adaptations enhance biofilm robustness, offering potential targets for disrupting polymicrobial biofilm persistence in clinical settings.

Conclusion

In conclusion, this study demonstrated the intricate interplay between *S. aureus* and *C. albicans* in polymicrobial biofilms, highlighting the critical role of nutrient environments, colonization order, and structural adaptations in shaping biofilm composition and resilience. Notably, the biofilm matrix emerged as a key modulator of biofilm dynamics, influencing interspecies interactions and the proliferation characteristics of individual strains. In particular, the stage-specific contribution of *C. albicans* hyphae to biofilm structure—supportive during maturation yet potentially suppressive during dispersion—emphasizes the dynamic complexity of interspecies interactions. These nuances further support the need for phase-tailored strategies in targeting persistent polymicrobial biofilms. Although variations in matrix composition were not the primary factor affecting total biofilm biomass, the strain-specific responses to different matrix types suggest its contribution to biofilm heterogeneity and adaptive potential. The enhanced shear resistance observed in matured biofilms, driven by *S. aureus* dominance and the promotion of *C. albicans* hyphae, underscored the challenges of eradicating chronic polymicrobial infections. These findings provide valuable insights into the mechanisms underlying biofilm persistence and offer potential avenues for developing targeted strategies to disrupt their formation and resilience in clinical settings.

Ethics Statement

The study was reviewed by the Jinan University Ethic Review Committee (20200826-02), Guangzhou, China and the research contents and methods were in line with the

medical ethics norms and requirements. Informed consent to human research participant in the study was obtained.

Acknowledgements

This work was supported by the National Natural Science Foundation of China [grant numbers, 32472465, 32202199], Guangdong Province Higher Education Featured Innovation Project [grant numbers, 2023KTSCX053], the Open Research Fund of State Key Laboratory of Biological Fermentation Engineering of Beer [grant numbers, K202105] and the 111 Project [grant numbers, B17018].

CRediT authorship contribution statement

Yaqin Li: Methodology, Investigation, Formal analysis, Data curation, Writing – original draft. Xiang Zhou: Conceptualization, Writing – review & editing, Supervision. Haoyue Xue: Formal analysis, Data curation. Jiaying Hong: Methodology, Investigation. Nixuan Gu: Methodology, Data curation. Qian Li: Investigation. Guangchao Yu: Writing – review & editing. Xiaomao Yin: Formal analysis. Lei Yuan: Investigation. Mahesh Premarathna: Formal analysis. Xin Lin: Methodology. Yuzhu Mao: Data curation. Junyan Liu: Conceptualization, Resources, Investigation, Writing – review & editing, Supervision. Zhenbo Xu: Conceptualization, Resources, Methodology, Investigation, Writing – review & editing, Supervision.

Declaration of interests

The authors declare that they have no known competing financial interests or personal relationships that could have appeared to influence the work reported in this paper.

Data availability

Data will be made available on request.

References

Allison, D. L., Scheres, N., Willems, H. M. E., Bode, C. S., Krom, B. P., & Shirtliff, M. E. (2019). The Host Immune System Facilitates Disseminated Staphylococcus aureus Disease Due to Phagocytic Attraction to Candida albicans during Coinfection: a Case of Bait and Switch. *Infect Immun, 87*(11). https://doi.org/10.1128/iai.00137-19.

Brogden, K. A., Guthmiller, J. M., & Taylor, C. E. (2005). Human polymicrobial infections. *Lancet, 365*(9455), 253-255. https://doi.org/10.1016/s0140-6736(05)17745-9.

Burmølle, M., Thomsen, T. R., Fazli, M., Dige, I., Christensen, L., Homøe, P., et al. (2010). Biofilms in chronic infections - a matter of opportunity - monospecies biofilms in multispecies infections. *FEMS Immunol Med Microbiol, 59*(3), 324-336. https://doi.org/10.1111/j.1574-695X.2010.00714.x.

Burmølle, M., Thomsen, T. R., Fazli, M., Dige, I., Christensen, L., Homøe, P., et al. (2010). Biofilms in chronic infections – a matter of opportunity – monospecies biofilms in multispecies infections. *FEMS Immunology & Medical Microbiology, 59*(3), 324-336. https://doi.org/10.1111/j.1574-695X.2010.00714.x %J FEMS Immunology & Medical Microbiology.

Carlson, E. (1982). Synergistic effect of Candida albicans and Staphylococcus aureus on mouse mortality. *Infect Immun, 38*(3), 921-924. https://doi.org/10.1128/iai.38.3.921-924.1982.

Chow, E. W. L., Pang, L. M., & Wang, Y. (2021). From Jekyll to Hyde: The Yeast–

Hyphal Transition of Candida albicans. *10*(7), 859.

Costerton, J. W., Stewart, P. S., & Greenberg, E. P. (1999). Bacterial biofilms: a common cause of persistent infections. *Science, 284*(5418), 1318-1322. https://doi.org/10.1126/science.284.5418.1318.

Gabrilska, R. A., & Rumbaugh, K. P. (2015). Biofilm models of polymicrobial infection. *Future Microbiol, 10*(12), 1997-2015. https://doi.org/10.2217/fmb.15.109.

Harriott, M. M., & Noverr, M. C. (2009). Candida albicans and Staphylococcus aureus form polymicrobial biofilms: effects on antimicrobial resistance. *Antimicrob Agents Chemother, 53*(9), 3914-3922. https://doi.org/10.1128/aac.00657-09.

Heitman, J. (2006). *Molecular principles of fungal pathogenesis*: Wiley Online Library.

Høiby, N., Bjarnsholt, T., Moser, C., Bassi, G. L., Coenye, T., Donelli, G., et al. (2015). ESCMID∗ guideline for the diagnosis and treatment of biofilm infections 2014. *Clinical Microbiology and Infection, 21*, S1-S25. https://doi.org/https://doi.org/10.1016/j.cmi.2014.10.024.

Hoiby, N., Flensborg, E. W., Beck, B., Friis, B., Jacobsen, S. V., & Jacobsen, L. (1977). Pseudomonas aeruginosa infection in cystic fibrosis. Diagnostic and prognostic significance of Pseudomonas aeruginosa precipitins determined by means of crossed immunoelectrophoresis. *Scand J Respir Dis, 58*(2), 65-79.

Jing, Q., Liu, R., Jiang, Q., Liu, Y., He, J., Zhou, X., et al. (2024). Staphylococcus aureus wraps around Candida albicans and synergistically escapes from Neutrophil extracellular traps. [Original Research]. *15*. https://doi.org/10.3389/fimmu.2024.1422440.

579 Kean, R., Rajendran, R., Haggarty, J., Townsend, E. M., Short, B., Burgess, K. E., et al.
580 (2017). Candida albicans Mycofilms Support Staphylococcus aureus
581 Colonization and Enhances Miconazole Resistance in Dual-Species Interactions.
582 [Original Research]. *8*. https://doi.org/10.3389/fmicb.2017.00258.
583 Kong Eric, F., Tsui, C., Kucharíková, S., Andes, D., Van Dijck, P., & Jabra-Rizk Mary,
584 A. (2016). Commensal Protection of Staphylococcus aureus against
585 Antimicrobials by Candida albicans Biofilm Matrix. *mBio, 7*(5),
586 10.1128/mbio.01365-01316. https://doi.org/10.1128/mbio.01365-16.
587 Lu, Y., Su, C., Solis, Norma V., Filler, Scott G., & Liu, H. (2013). Synergistic
588 Regulation of Hyphal Elongation by Hypoxia, CO2, and Nutrient Conditions
589 Controls the Virulence of Candida albicans. *Cell Host & Microbe, 14*(5), 499-
590 509. https://doi.org/https://doi.org/10.1016/j.chom.2013.10.008.
591 Lu, Y., Su, C., Wang, A., & Liu, H. (2011). Hyphal Development in Candida albicans
592 Requires Two Temporally Linked Changes in Promoter Chromatin for Initiation
593 and Maintenance. *PLOS Biology, 9*(7), e1001105.
594 https://doi.org/10.1371/journal.pbio.1001105.
595 Luo, G., Wang, T., Zhang, J., Zhang, P., & Lu, Y. (2021). Candida albicans requires iron
596 to sustain hyphal growth. *Biochemical and Biophysical Research*
597 *Communications, 561*, 106-112.
598 https://doi.org/https://doi.org/10.1016/j.bbrc.2021.05.039.
599 Ma, R., Hu, X., Zhang, X., Wang, W., Sun, J., Su, Z., et al. (2022). Strategies to prevent,
600 curb and eliminate biofilm formation based on the characteristics of various

periods in one biofilm life cycle. [Review]. *12*. https://doi.org/10.3389/fcimb.2022.1003033.

Moormeier, D. E., & Bayles, K. W. (2017). Staphylococcus aureus biofilm: a complex developmental organism. *104*(3), 365-376. https://doi.org/https://doi.org/10.1111/mmi.13634.

Nash, E. E., Peters, B. M., Palmer, G. E., Fidel, P. L., & Noverr, M. C. (2014). Morphogenesis Is Not Required for Candida albicans-Staphylococcus aureus Intra-Abdominal Infection-Mediated Dissemination and Lethal Sepsis. *82*(8), 3426-3435. https://doi.org/doi:10.1128/iai.01746-14.

Odds, F. C. (1988). *Candida and candidosis: a review and bibliography*.

Pasman R, Krom BP, Jonker MJ, de Leeuw WC, Kramer G, Brul S, et al. (2025) Candida albicans and Staphylococcus aureus reciprocally promote their virulence factor secretion and pro-inflammatory effects. Front Cell Infect Microbiol. 15:1629373. https://doi.org/ 10.3389/fcimb.2025.1629373.

Paul, S., Todd, O. A., Eichelberger, K. R., Tkaczyk, C., Sellman, B. R., Noverr, M. C., et al. (2024). A fungal metabolic regulator underlies infectious synergism during Candida albicans-Staphylococcus aureus intra-abdominal co-infection. *Nature Communications, 15*(1), 5746. https://doi.org/10.1038/s41467-024-50058-w.

Peleg, A. Y., Hogan, D. A., & Mylonakis, E. (2010). Medically important bacterial–fungal interactions. *Nature Reviews Microbiology, 8*(5), 340-349. https://doi.org/10.1038/nrmicro2313.

Schlecht, L. M., Peters, B. M., Krom, B. P., Freiberg, J. A., Hänsch, G. M., Filler, S. G.,

et al. (2015). Systemic Staphylococcus aureus infection mediated by Candida albicans hyphal invasion of mucosal tissue. *Microbiology (Reading), 161*(Pt 1), 168-181. https://doi.org/10.1099/mic.0.083485-0.

Shao, T.-Y., Ang, W. X. G., Jiang, T. T., Huang, F. S., Andersen, H., Kinder, J. M., et al. (2019). Commensal Candida albicans Positively Calibrates Systemic Th17 Immunological Responses. *Cell Host & Microbe, 25*(3), 404-417.e406. https://doi.org/https://doi.org/10.1016/j.chom.2019.02.004.

Shao, T. Y., Ang, W. X. G., Jiang, T. T., Huang, F. S., Andersen, H., Kinder, J. M., et al. (2019). Commensal Candida albicans Positively Calibrates Systemic Th17 Immunological Responses. *Cell Host Microbe, 25*(3), 404-417.e406. https://doi.org/10.1016/j.chom.2019.02.004.

Stepanović, S., Vuković, D., Hola, V., Di Bonaventura, G., Djukić, S., Cirković, I., et al. (2007). Quantification of biofilm in microtiter plates: overview of testing conditions and practical recommendations for assessment of biofilm production by staphylococci. *Apmis, 115*(8), 891-899. https://doi.org/10.1111/j.1600-0463.2007.apm_630.x.

Stoodley, P., Sauer, K., Davies, D. G., & Costerton, J. W. (2002). Biofilms as Complex Differentiated Communities. *56*(Volume 56, 2002), 187-209. https://doi.org/https://doi.org/10.1146/annurev.micro.56.012302.160705.

Todd Olivia, A., Fidel Paul, L., Harro Janette, M., Hilliard Jamese, J., Tkaczyk, C., Sellman Bret, R., et al. (2019). Candida albicans Augments Staphylococcus aureus Virulence by Engaging the Staphylococcal agr Quorum Sensing System.

mBio, 10(3), 10.1128/mbio.00910-00919. https://doi.org/10.1128/mbio.00910-19.

Van Dyck, K., Viela, F., Mathelié-Guinlet, M., Demuyser, L., Hauben, E., Jabra-Rizk, M. A., et al. (2021). Adhesion of Staphylococcus aureus to Candida albicans During Co-Infection Promotes Bacterial Dissemination Through the Host Immune Response. [Original Research]. *10*. https://doi.org/10.3389/fcimb.2020.624839.

Vila, T., Kong, E. F., Montelongo-Jauregui, D., Van Dijck, P., Shetty, A. C., McCracken, C., et al. (2021). Therapeutic implications of *C. albicans-S. aureus* mixed biofilm in a murine subcutaneous catheter model of polymicrobial infection. *Virulence, 12*(1), 835-851. https://doi.org/10.1080/21505594.2021.1894834.

Vylkova, S., Carman Aaron, J., Danhof Heather, A., Collette John, R., Zhou, H., & Lorenz Michael, C. (2011). The Fungal Pathogen Candida albicans Autoinduces Hyphal Morphogenesis by Raising Extracellular pH. *mBio, 2*(3), 10.1128/mbio.00055-00011. https://doi.org/10.1128/mbio.00055-11.

Willems, H. M., Xu, Z., & Peters, B. M. (2016). Polymicrobial Biofilm Studies: From Basic Science to Biofilm Control. *Curr Oral Health Rep, 3*(1), 36-44. https://doi.org/10.1007/s40496-016-0078-y.

Wolcott, R., Costerton, J. W., Raoult, D., & Cutler, S. J. (2013). The polymicrobial nature of biofilm infection. *Clin Microbiol Infect, 19*(2), 107-112. https://doi.org/10.1111/j.1469-0691.2012.04001.x.

Xu, Z., Liang, Y., Lin, S., Chen, D., Li, B., Li, L., et al. (2016). Crystal Violet and XTT

667 Assays on Staphylococcus aureus Biofilm Quantification. *Curr Microbiol, 73*(4), 474-482. https://doi.org/10.1007/s00284-016-1081-1.

669 Yang, D., Zhang, M., Su, C., Dong, B., & Lu, Y. (2023). Candida albicans exploits N-acetylglucosamine as a gut signal to establish the balance between commensalism and pathogenesis. *Nature Communications, 14*(1), 3796. https://doi.org/10.1038/s41467-023-39284-w.

673

674 **Table 1** Clinical isolates of 24 pairs of *S. aureus* and *C. albicans*.

Group	Strain No.		Source	Clinical origin	Co-isolated Strains	Strain Designations
Pair 1	Calb191264	Saur191264	Sputum	Neurology	*C. albicans* +; MRSA +	Ca-1+Sa-1
Pair2	Calb192203	Saur192203	Sputum	/	*C. albicans* +; MRSA ++	Ca-2+Sa-2
Pair3	Calb190201	Saur190201	Sputum	Nephrology	*C. albicans* +; MRSA +	Ca-3+Sa-3
Pair4	Calb190476	Saur190476	Sputum	Pediatrics	*C. albicans* +; MRSA +	Ca-4+Sa-4
Pair5	Calb191045	Saur191045	Sputum	Traditional Chinese Medicine	*C. albicans* +; MRSA +	Ca-5+Sa-5
Pair6	Calb192031	Saur192031	Sputum	Neurosurgery	*C. albicans* +; MRSA +	Ca-6+Sa-6
Pair7	Calb192315	Saur192315	Sputum	Oncology	*C. albicans* +++; MRSA +	Ca-7+Sa-7
Pair8	Calb192707	Saur192707	Sputum	Neurology	*C. albicans* +; MRSA +	Ca-8+Sa-8
Pair9	Calb193012	Saur193012	Sputum	Intensive Care Unit (ICU)	*C. albicans* +; MRSA ++	Ca-9+Sa-9
Pair10	Calb191053	Saur191053	Sputum	Neurosurgery	*C. albicans* ++; MRSA +	Ca-10+Sa-10
Pair11	Calb191630	Saur191630	Sputum	Cardiology	*C. albicans* +; MRSA ++	Ca-11+Sa-11
Pair12	Calb191639	Saur191639	Sputum	Nephrology	*C. albicans* +; MRSA +	Ca-12+Sa-12
Pair13	Calb190214	Saur190214	Sputum	Neurology	*C. albicans* ++; MRSA +	Ca-13+Sa-13
Pair14	Calb190631	Saur190631	Sputum	Neurology	*C. albicans* +; MRSA +	Ca-14+Sa-14
Pair15	Calb191146	Saur191146	Sputum	ICU	*C. albicans* +; MRSA +	Ca-15+Sa-15
Pair16	Calb190245	Saur190245	Sputum	Pediatrics	*C. albicans* ++; MRSA +	Ca-16+Sa-16
Pair17	Calb191313	Saur191313	Sputum	Oncology	*C. albicans* +; MRSA ++	Ca-17+Sa-17
Pair18	Calb191852	Saur191852	Sputum	ICU	*C. albicans* ++; MRSA ++	Ca-18+Sa-18
Pair19	Calb192143	Saur192143	Sputum	Neonatology	*C. albicans* ++; MRSA +	Ca-19+Sa-19
Pair20	Calb192149	Saur192149	Sputum	Respiratory Medicine	*C. albicans* ++; MRSA +	Ca-20+Sa-20
Pair21	Calb190621	Saur190621	Urine	Urologic Surgery	*C. albicans* +; MRSA +	Ca-21+Sa-21
Pair22	Calb190801	Saur190801	Sputum	Gastrointestinal Surgery	*C. albicans* +; MRSA +	Ca-22+Sa-22
Pair23	Calb191210	Saur191210	Sputum	Oncology	*C. albicans* ++; MRSA +	Ca-23+Sa-23
Pair24	Calb190246	Saur190246	Sputum	Respiratory Medicine	*C. albicans* +; MRSA +	Ca-24+Sa-24

675 Biofilm forming ability: + weak; ++ medium; +++ strong

676

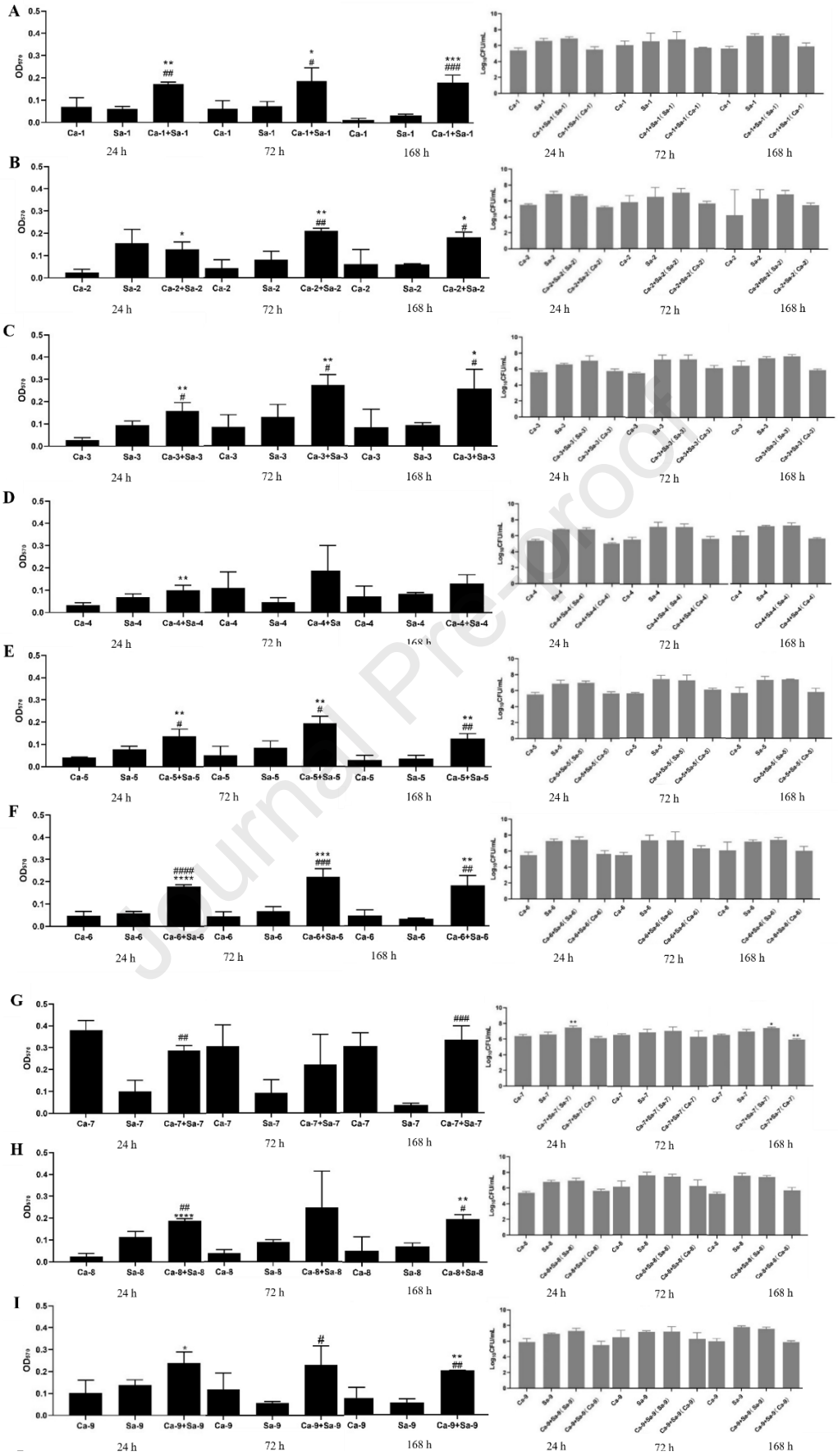

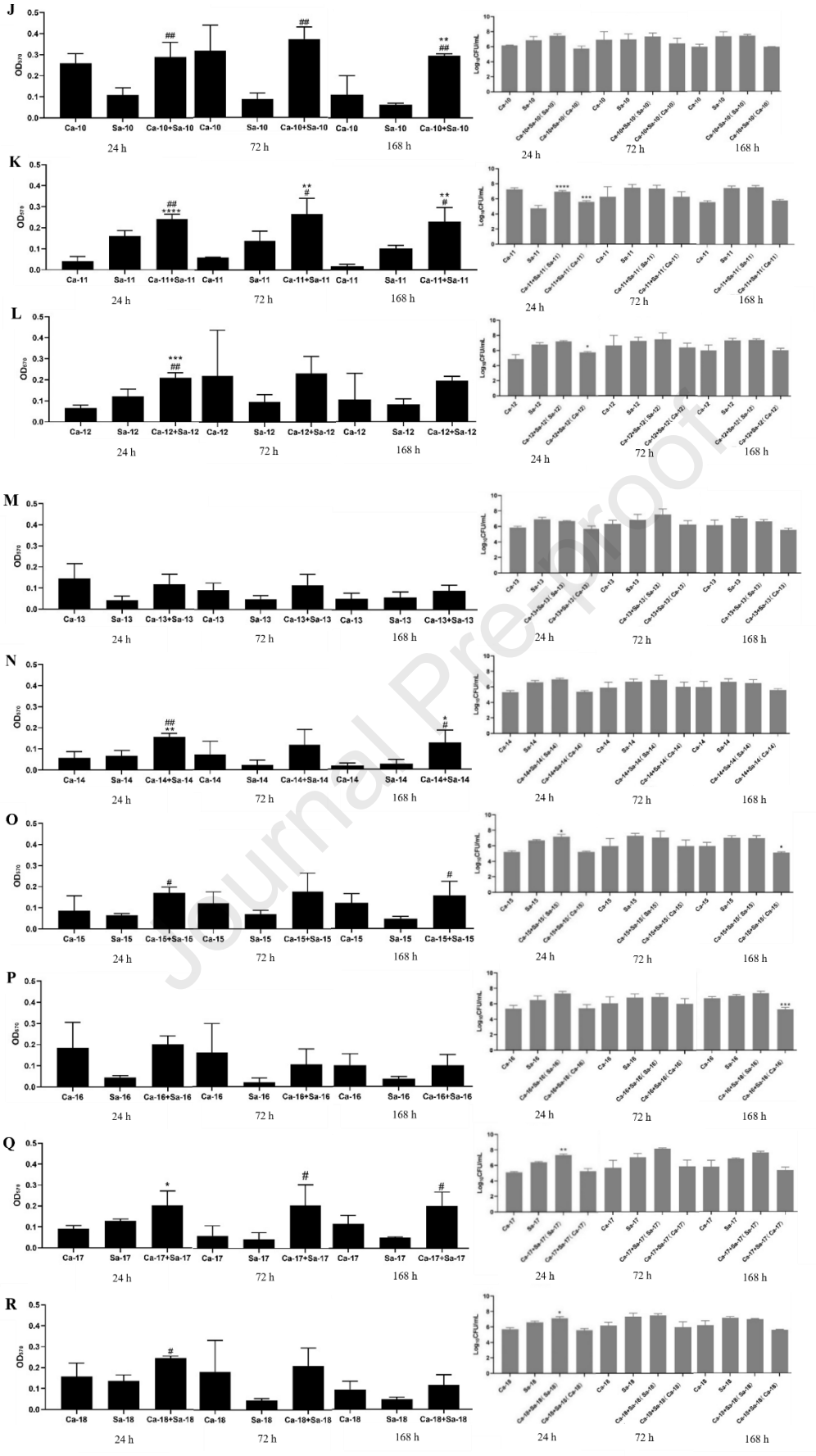

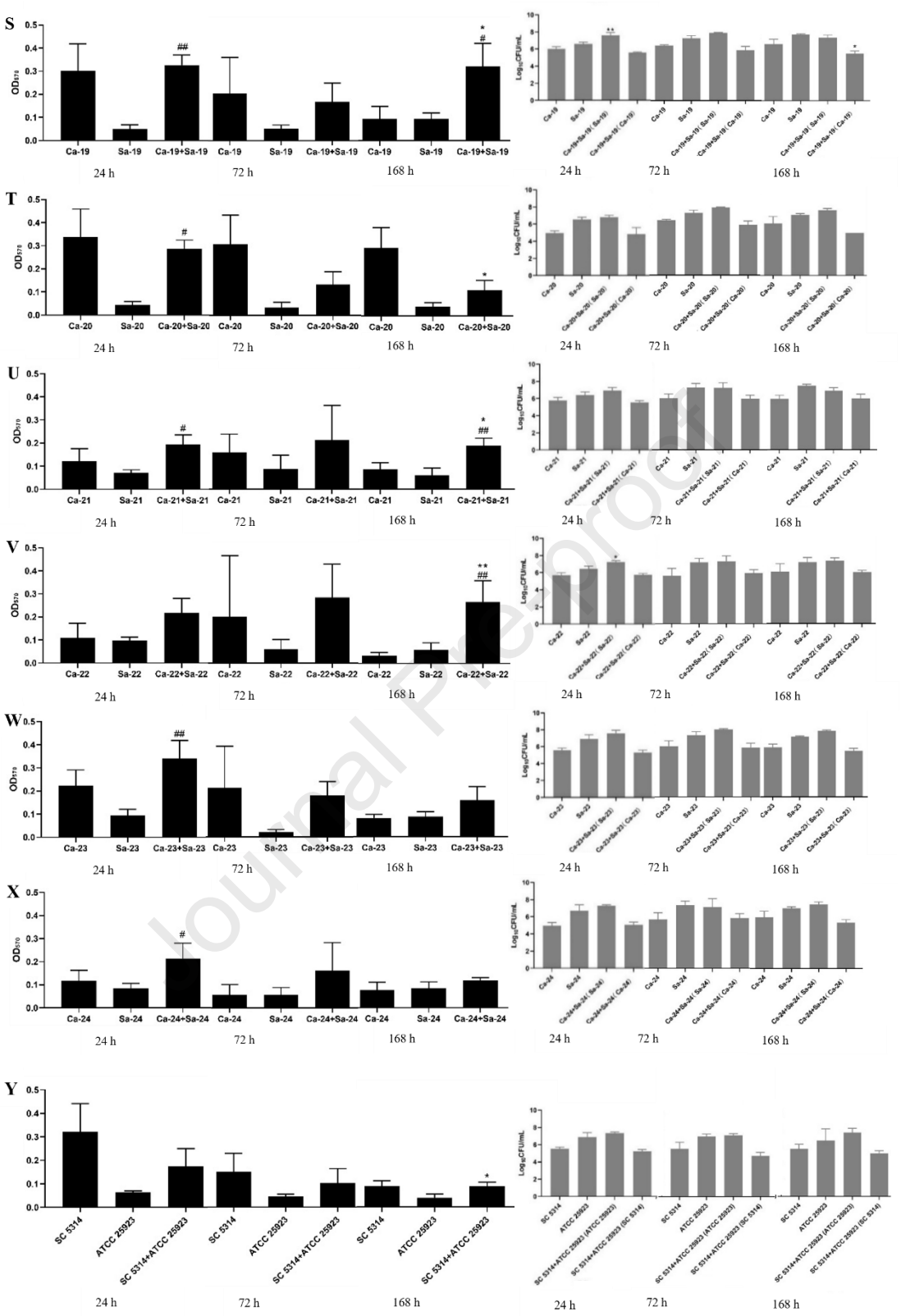

Figure 1 Dual species biofilm of *S. aureus* and *C. albicans* (in hyphae). Data include both monoculture biofilms (*S. aureus* or *C. albicans* alone) and dual-species biofilms, allowing direct comparison of biofilm characteristics under identical experimental conditions.

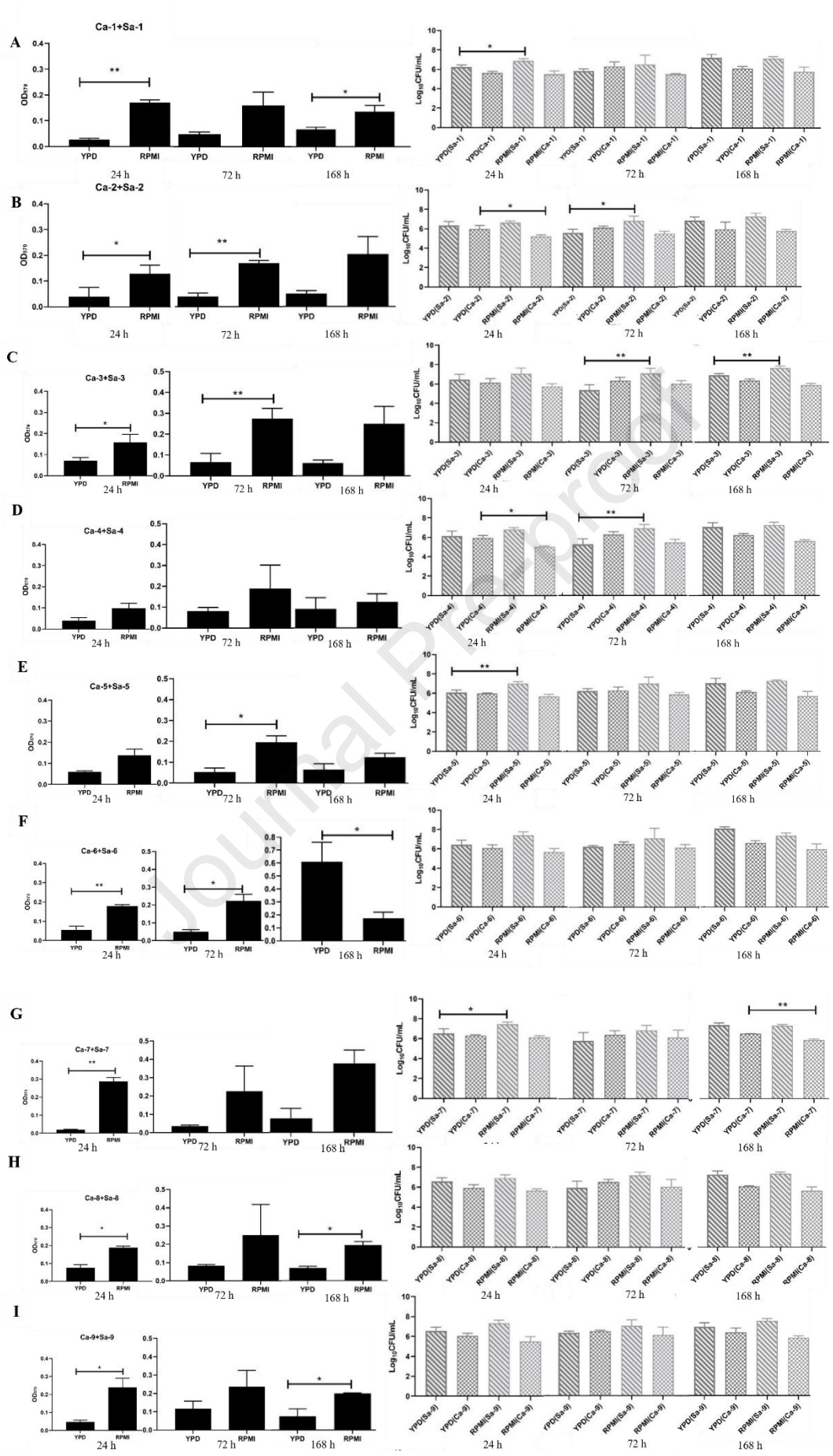

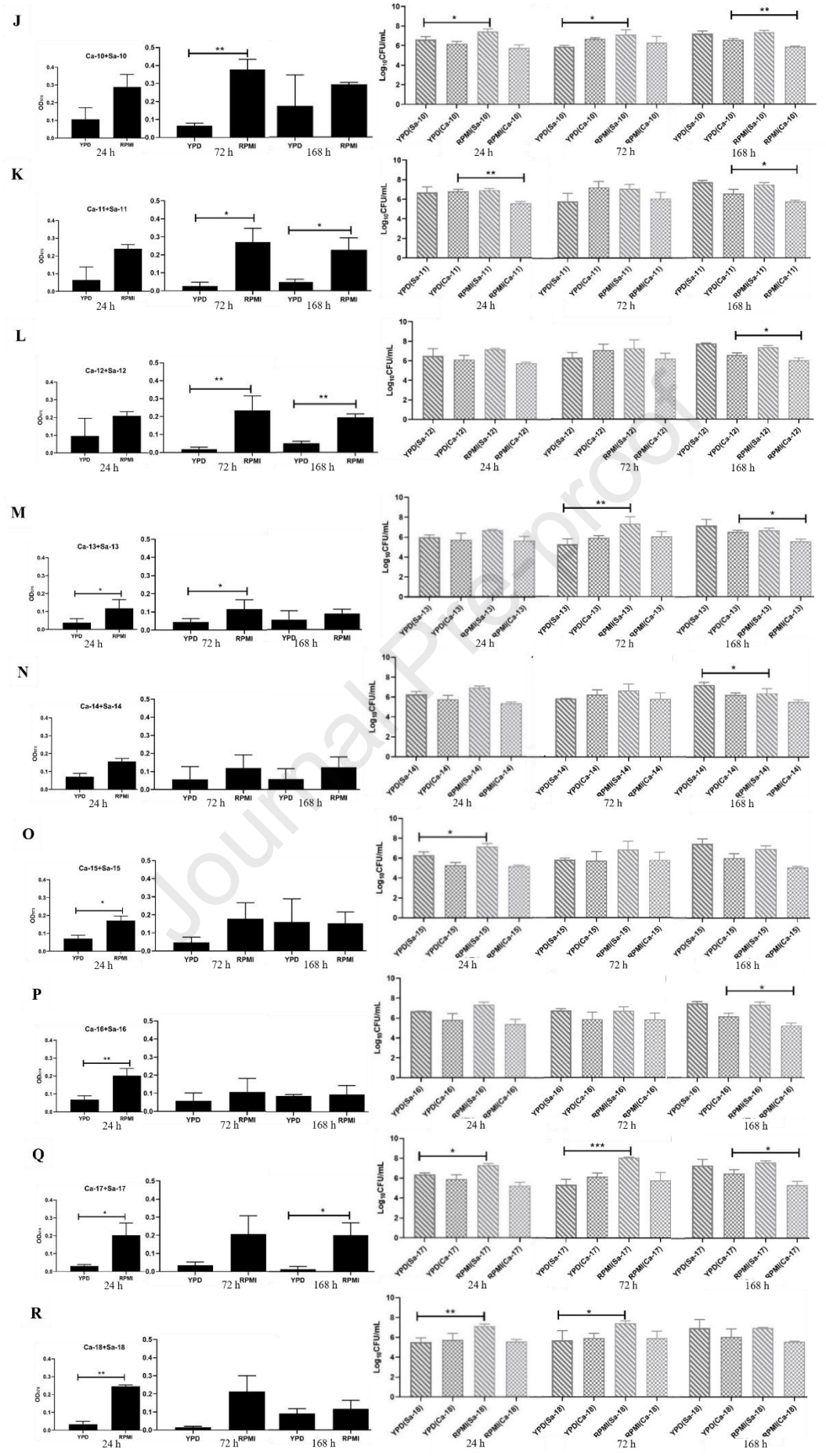

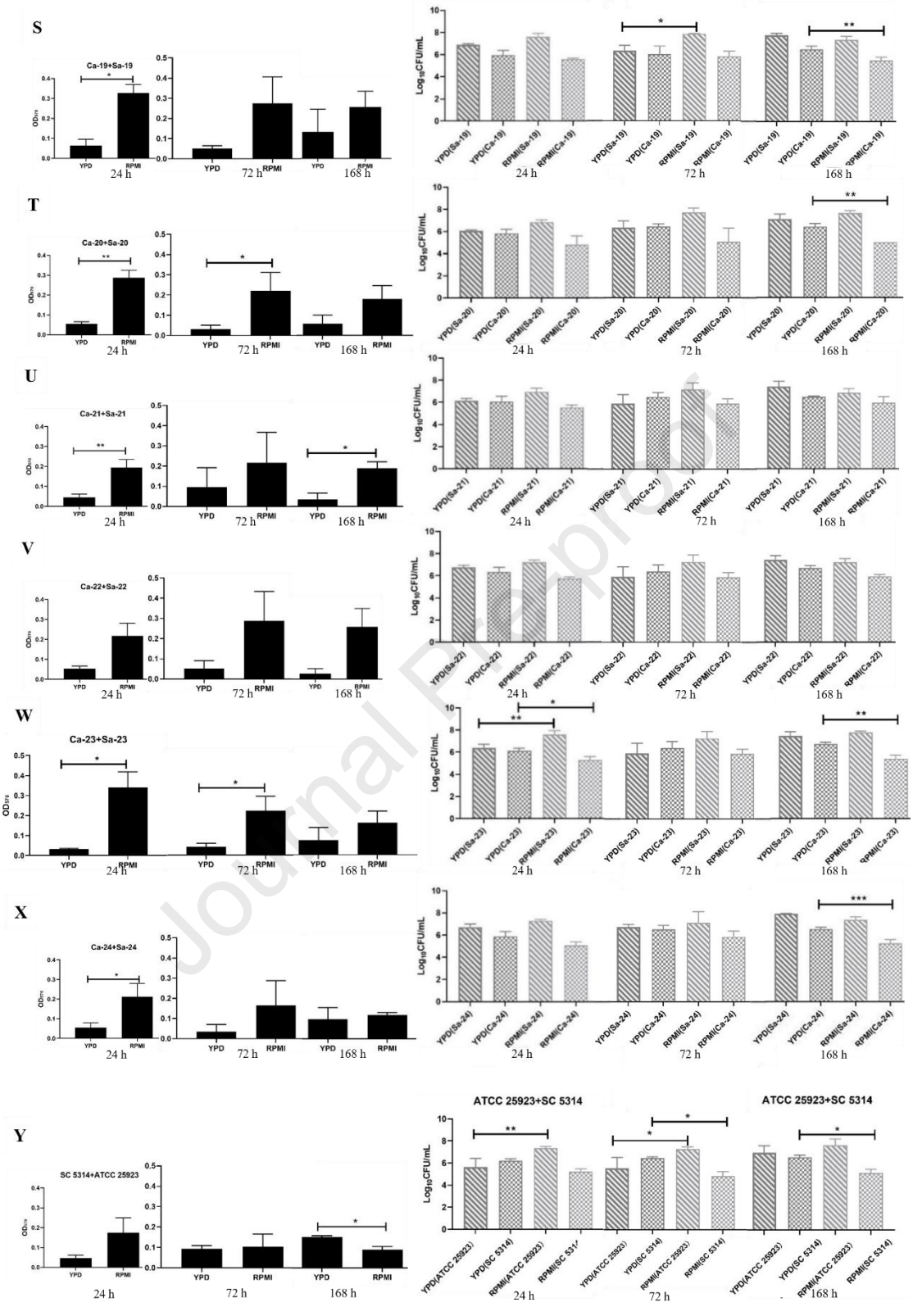

Figure 2 Dual species biofilm of *S. aureus*-*C. albicans* in yeast and hyphae.

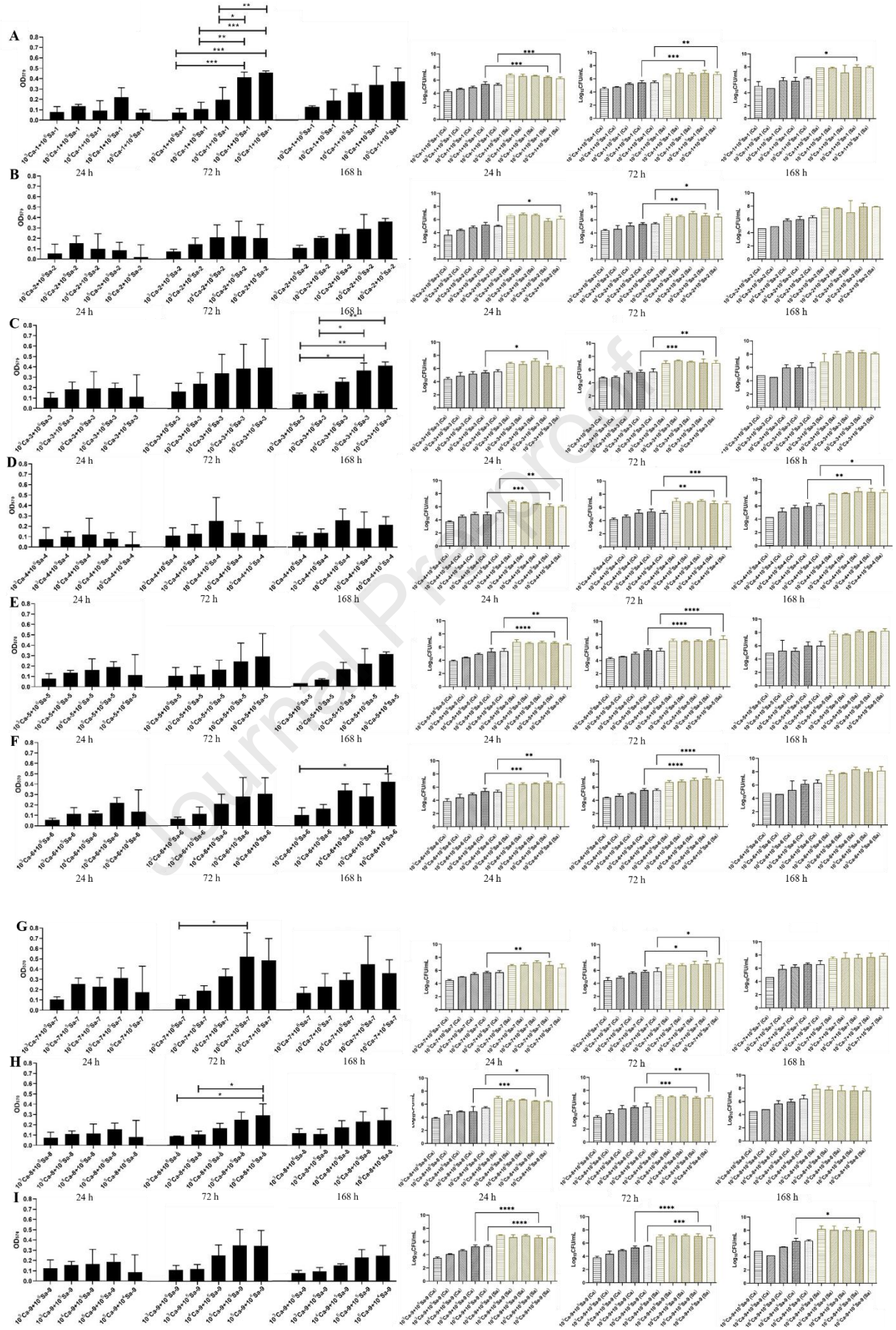

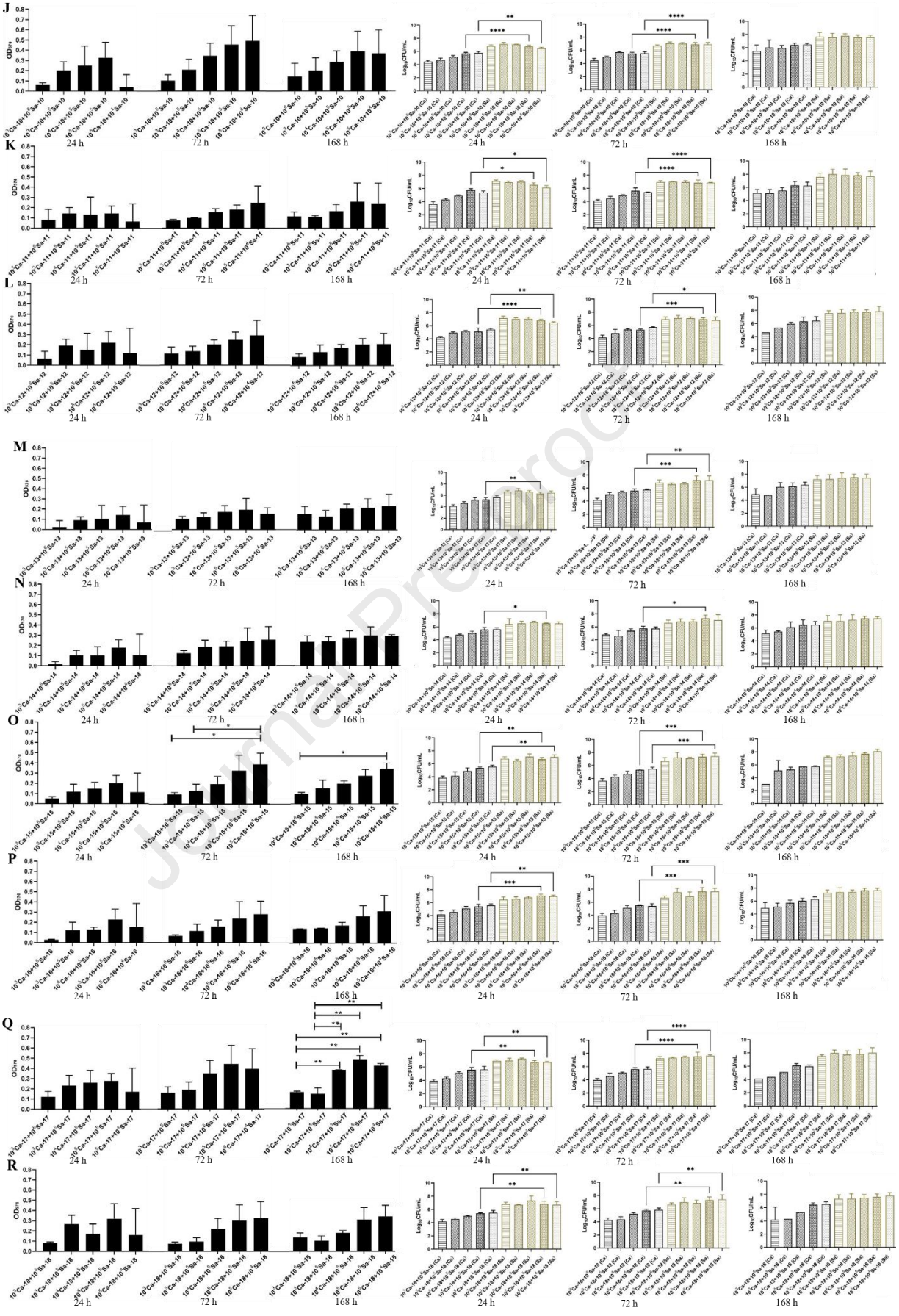

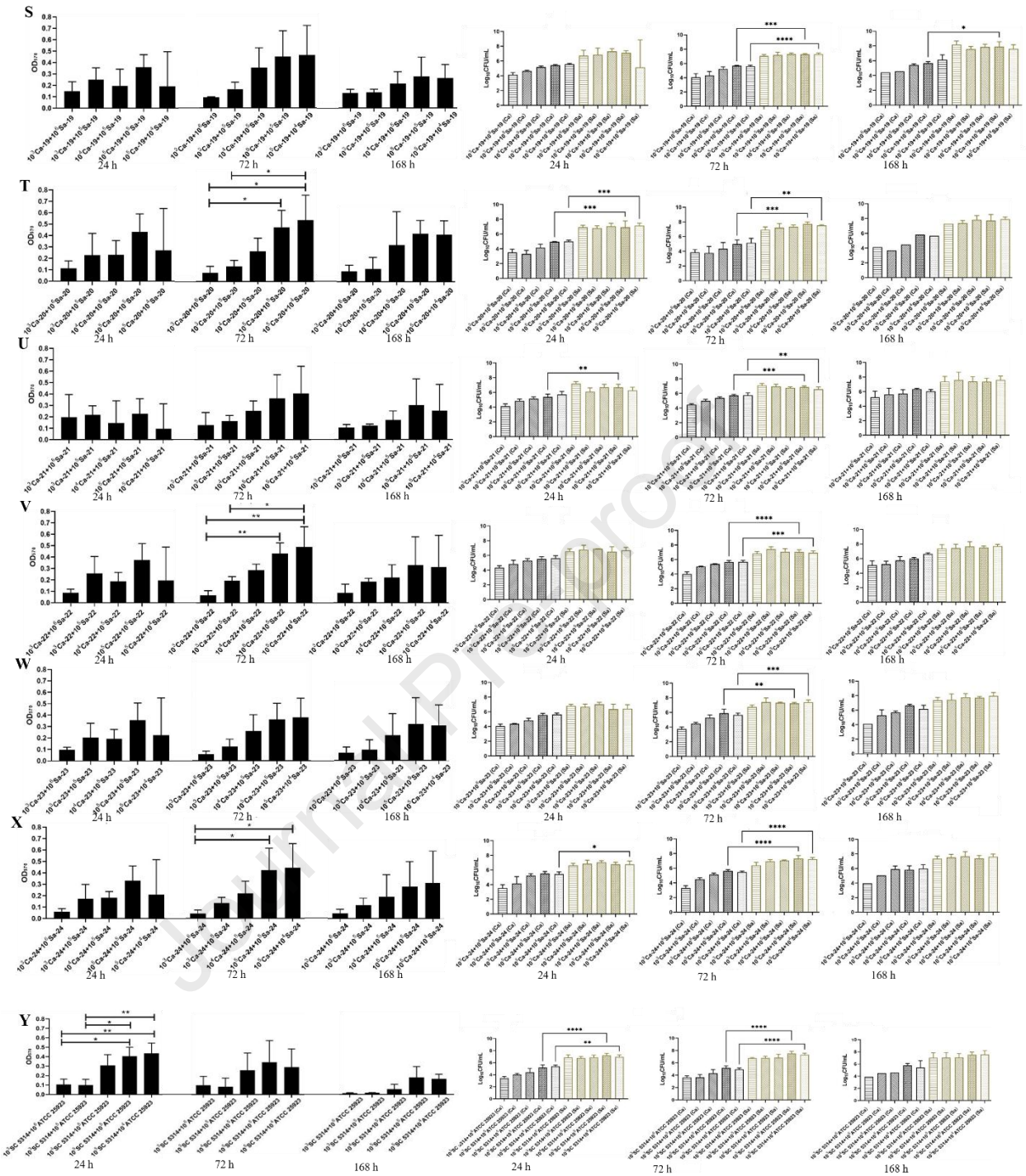

Figure 3 Dual species biofilm of *S. aureus*-*C. albicans* under different initial inoculation concentration.

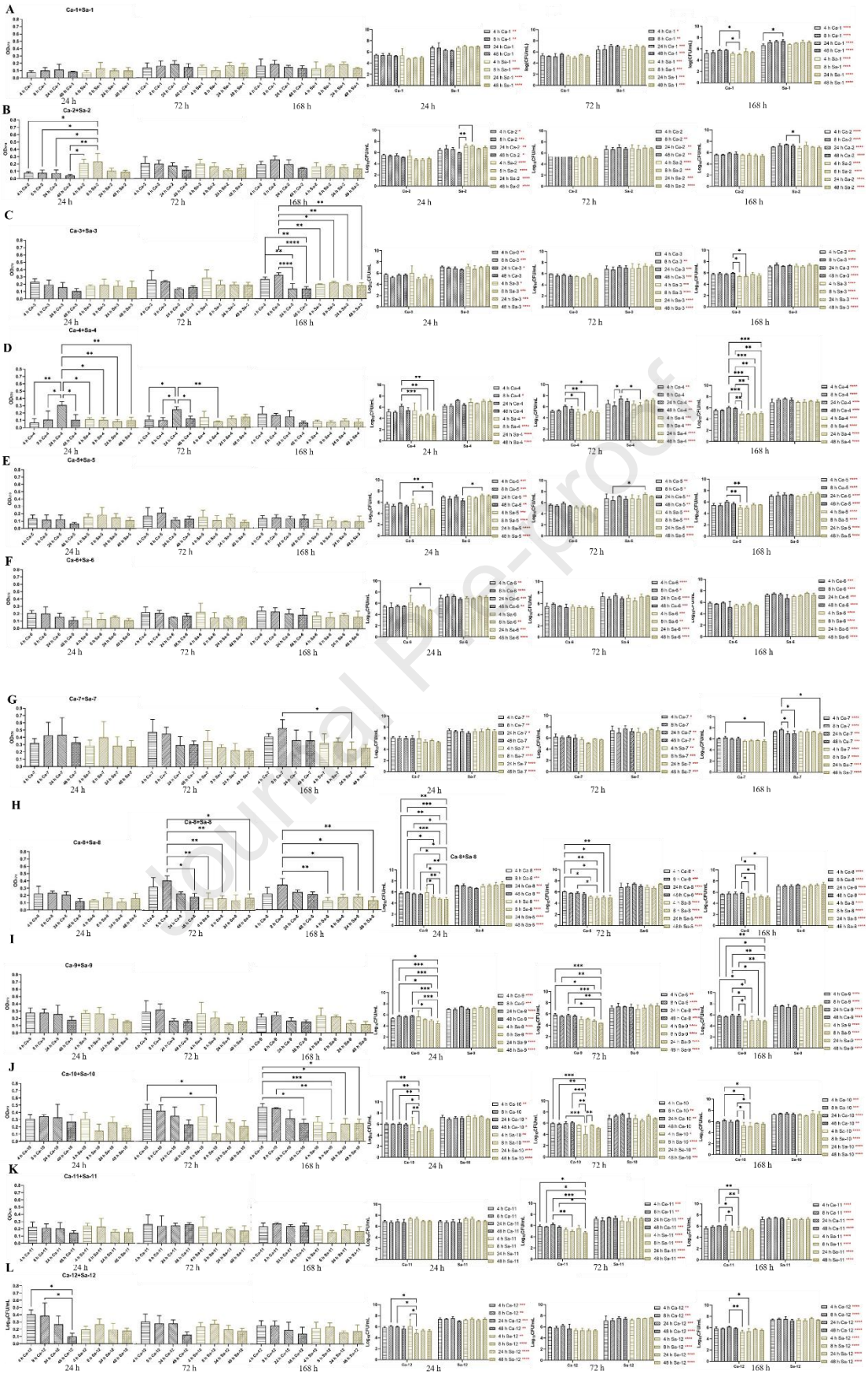

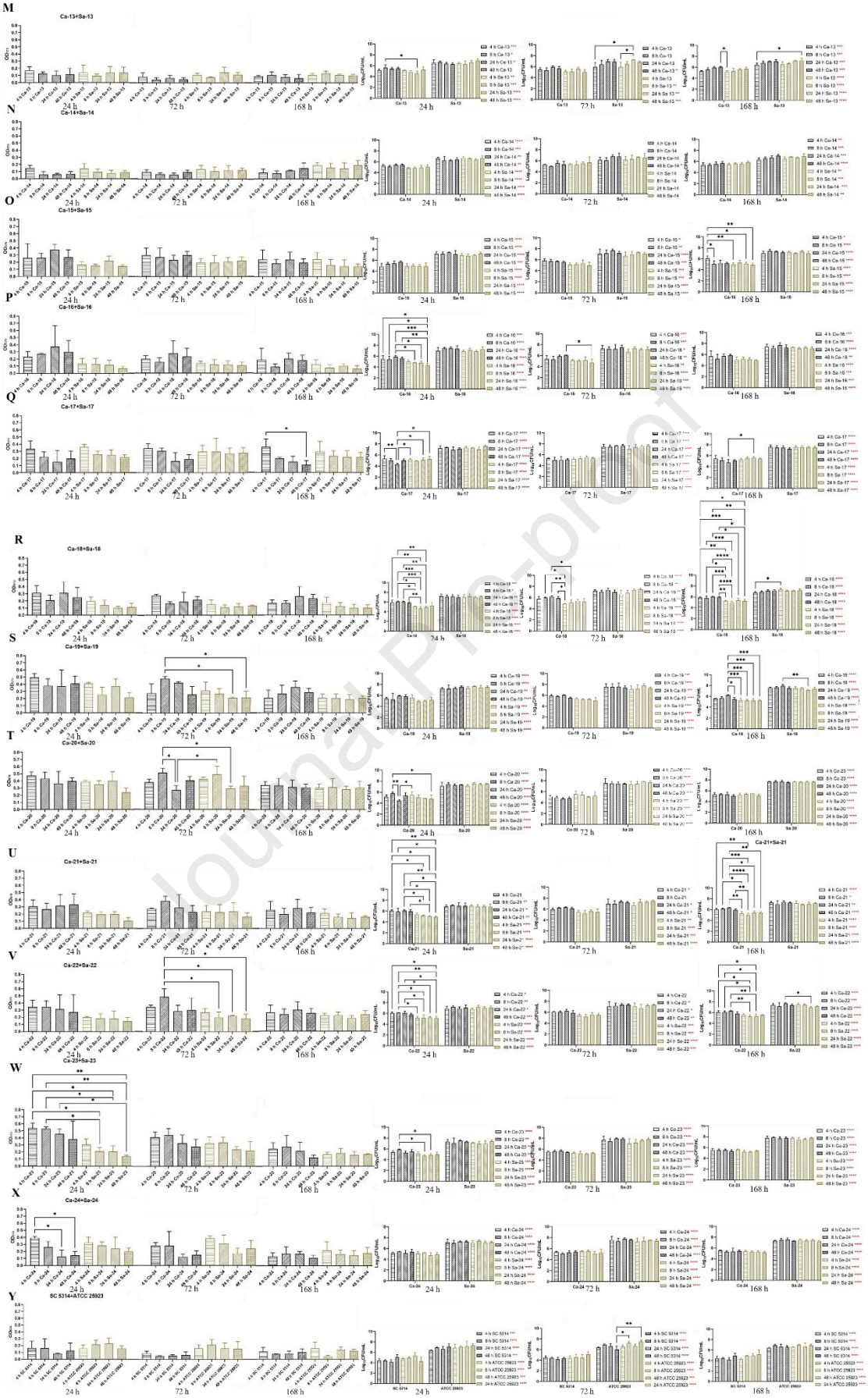

Figure 4 Dual species biofilm of *S. aureus*-*C. albicans* under different growth order.

A

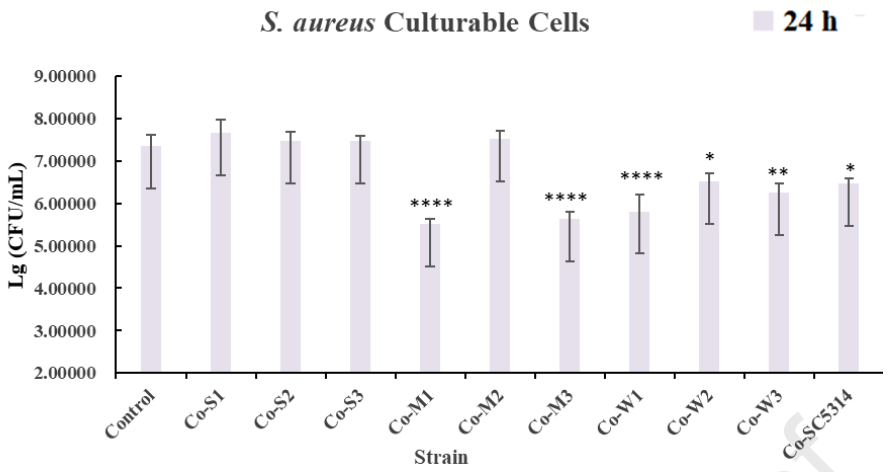

B

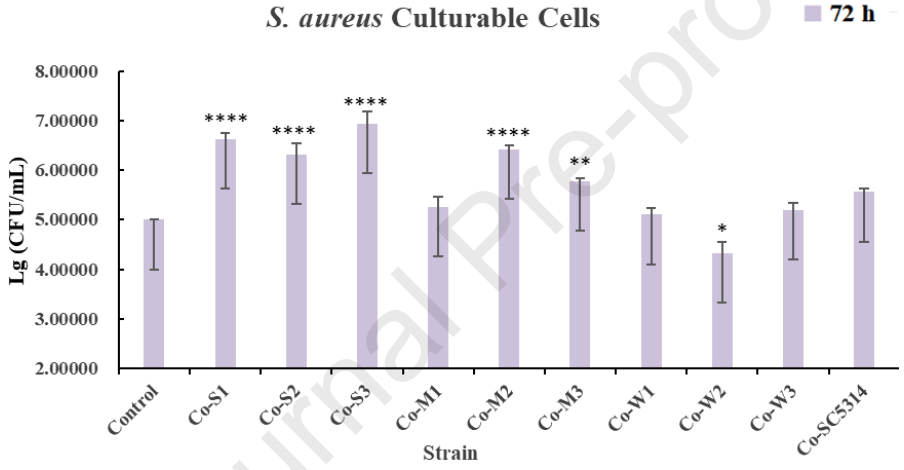

C

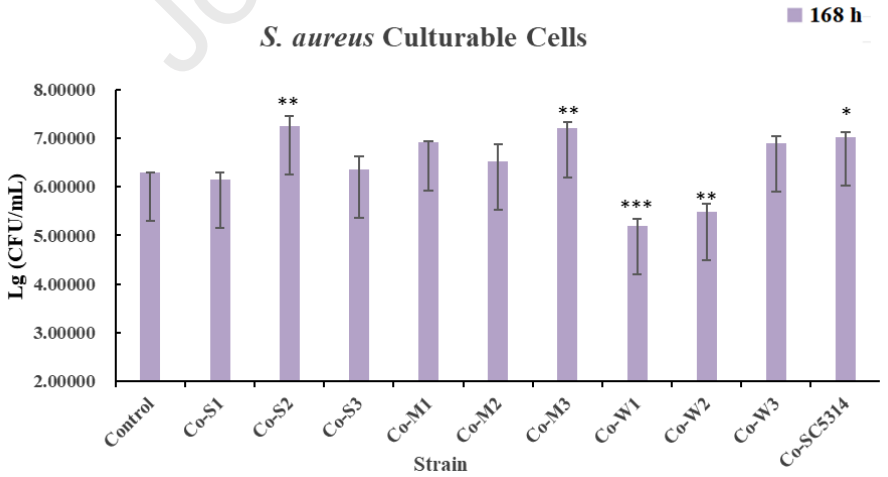

Figure 5 *S. aureus* cells in polymicrobial biofilms formed with *C. albicans* strains exhibiting strong, moderate, and weak hyphal-forming abilities at different time points.(A), (B), and (C) represent biofilms collected at 24 h, 72 h, and 168 h, respectively.

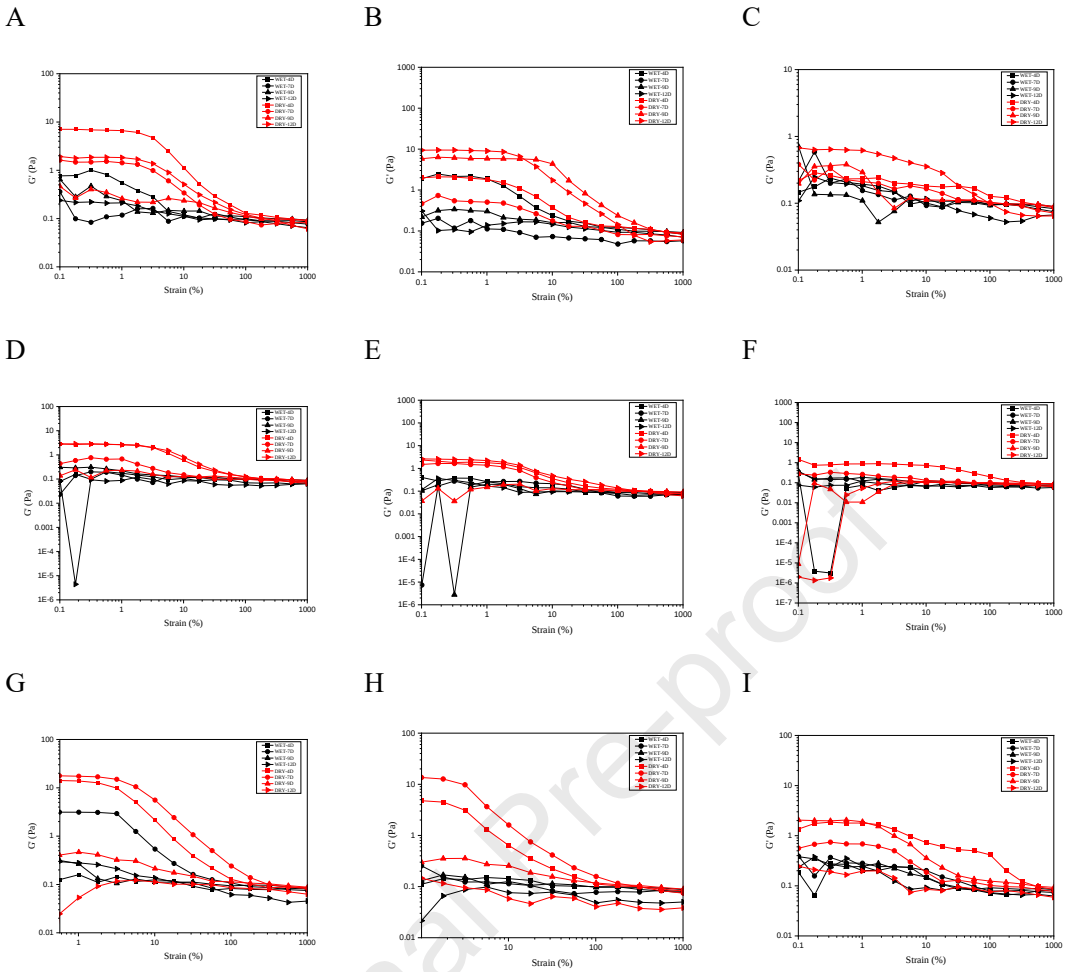

Figure 6 Amplitude sweep analysis of polymicrobial biofilms formed by *S. aureus* with strong (A, D, G), moderate (B, E, H), and weak (C, F, I) biofilm-forming abilities co-cultured with *C. albicans* strains exhibiting strong (A–C), moderate (D–F), and weak (G–I) hyphal-forming abilities.

Declaration of Interest Statement

The authors declare that they have no known competing financial interests or personal relationships that could have appeared to influence the work reported in this paper.